Article
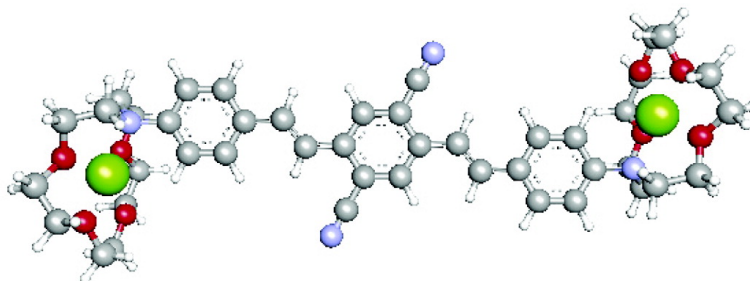
Metal-Ion Sensing Fluorophores with Large Two-Photon Absorption Cross Sections: Aza-Crown Ether Substituted Donor−Acceptor−Donor Distyrylbenzenes

Stephanie J. K. Pond, Osamu Tsutsumi, Mariacristina Rumi, Ohyun Kwon,
Egbert Zojer, Jean-Luc Brdas, Seth R. Marder, and Joseph W. Perry

More About This Article

Additional resources and features associated with this article are available within the HTML version:

- Supporting Information
- Links to the 14 articles that cite this article, as of the time of this article download
- Access to high resolution figures
- Links to articles and content related to this article
- Copyright permission to reproduce figures and/or text from this article

View the Full Text HTML

Metal-Ion Sensing Fluorophores with Large Two-Photon Absorption Cross Sections: Aza-Crown Ether Substituted Donor−Acceptor−Donor Distyrylbenzenes

Stephanie J. K. Pond,[†] Osamu Tsutsumi,[†,§] Mariacristina Rumi,[†,‡] Ohyun Kwon,[†,‡] Egbert Zojer,[†,‡] Jean-Luc Brédas,*,[†,‡] Seth R. Marder,*,[†,‡] and Joseph W. Perry*,[†,‡]

Contribution from the Department of Chemistry, University of Arizona, Tucson, Arizona 85721, and School of Chemistry and Biochemistry, Georgia Institute of Technology, Atlanta, Georgia 30332

Received February 20, 2004; E-mail: jean-luc.bredas@chemistry.gatech.edu; seth.marder@chemistry.gatech.edu; joe.perry@chemistry.gatech.edu

Abstract: Chromophores based on a donor−acceptor−donor structure possessing a large two-photon absorption cross section and one or two mono-aza-15-crown-5 ether moieties, which can bind metal cations, have been synthesized. The influence of Mg^{2+} binding on their one- and two-photon spectroscopic properties has been investigated. Upon binding, the two-photon action cross sections at 810 nm decrease by a factor of up to 50 at high Mg^{2+} concentrations and this results in a large contrast in the two-photon excited fluorescence signal between the bound and unbound forms, for excitation in the range of 730 to 860 nm. Experimental and computational results indicate that there is a significant reduction of the electron donating strength of the aza-crown nitrogen atom(s) upon metal ion binding and that this leads to a blue shift in the position as well as a reduction in the strength of the lowest-energy two-photon absorption band. The molecules reported here can serve as models for the design of improved two-photon excitable metal-ion sensing fluorophores.

Introduction

Two-photon laser scanning microscopy (TPLSM) is a powerful method for three-dimensional imaging in biological systems, and has been used to image the distribution of metal ions in living tissues.[1−3] In TPLSM, the ability of two-photon excitation to access excited states with photons of half the nominal excitation energy provides improved depth penetration in cell cultures and tissue specimens, which are scattering media, and reduces the background due to cellular autofluorescence, because the photons are detuned from resonance with native chromophores. Moreover, the dependence of the two-photon absorption probability on the square of the excitation intensity allows for excitation of chromophores with a high degree of spatial selectivity in three dimensions.[1] Currently, the fluorophores being used for TPLSM are largely those that have been developed for single-photon excitation.[4−7] Most of these conventional fluorophores have relatively small values of the two-photon absorption cross section, δ ($\sim$10 GM; 1 GM $\equiv$ 1×10^{-50} cm^4 s $photon^{-1}$ $molecule^{-1}$), or their optimal excitation wavelengths do not fall into the transmissive window for biological tissues, which lies between $\sim$600 and 1300 nm.[8,9] TPLSM could greatly benefit from the development of chromophores with large δ ($>$1000 GM) that can be excited efficiently in this range.

The need for improved two-photon chromophores has led in recent years to a significant amount of research that has been focused on the development of structure/property relationships for two-photon absorption. Various classes of two-photon chromophores have been investigated, including quasi-linear quadrupolar molecules symmetrically substituted with donor (D) and/or acceptor (A) groups (of the type D−π−D, A−π−A, D−A−D, and A−D−A) incorporating a variety of conjugated bridges,[10−14] bifluorene and polyfluorene systems,[15,16] various dipolar conjugated D−A molecules,[12,17,18] octupolar,[19,20] multi-

† Department of Chemistry, University of Arizona.
‡ School of Chemistry and Biochemistry, Georgia Institute of Technology.
§ Present address: Ebara Research, 4-2-1 Honfujisawa, Fujisawa 251-8502, Japan.

(1) Denk, W.; Piston, D. W.; Webb, W. W. In *Handbook of Biological Confocal Microscopy*; Pawley, J. B., Ed.; Plenum Press: New York, 1995; pp 445−458.
(2) Stosiek, C.; Garaschuk, O.; Holthoff, K.; Konnerth, A. *Proc. Nat. Acad. Sci.* **2003**, *100*, 7319−7324.
(3) Rubart, M.; Wang, E. X.; Dunn, K. W.; Field, L. J. *Am. J. Physiol. Cell Physiol.* **2003**, *284*, C1654−C1668.
(4) Brown, E. B.; Shear, J. B.; Adams, S. R.; Tsien, R. Y.; Webb, W. W. *Biophys. J.* **1999**, *76*, 489−499.
(5) Baker, G. A.; Munson, C. A.; Bukowski, E. J.; Baker, S. N.; Bright, F. V. *Appl. Spectrosc.* **2002**, *56*, 455−463.
(6) Koester, H. J.; Baur, D.; Uhl, R.; Hell, S. W. *Biophys. J.* **1999**, *77*, 2226−2236.
(7) Kuba, K.; Nakayama, S. *Neurosci. Res.* **1998**, *32*, 281−294.

(8) Fercher, A. F.; Drexler, W.; Hitzenbenger, C. K.; Lasser, T. *Rep. Prog. Phys.* **2003**, *66*, 239−303.
(9) Fisher, W. G.; Partridge, W. P., Jr.; Dees, C.; Wachter, E. A. *Photochem. Photobiol.* **1997**, *66*, 141−155.
(10) Albota, M.; Beljonne, D.; Brédas, J.-L.; Ehrlich, J. E.; Fu, J.-Y.; Heikal, A. A.; Hess, S. E.; Kogej, T.; Levin, M. D.; Marder, S. R.; McCord-Maughon, D.; Perry, J. W.; Röckel, H.; Rumi, M.; Subramaniam, G.; Webb, W. W.; Wu, X.-L.; Xu, C. *Science* **1998**, *281*, 1653−1656.
(11) Rumi, M.; Ehrlich, J. E.; Heikal, A. A.; Perry, J. W.; Barlow, S.; Hu, Z.; McCord-Maughon, D.; Parker, T. C.; Röckel, H.; Thayumanavan, S.; Marder, S. R.; Beljonne, D.; Brédas, J.-L. *J. Am. Chem. Soc.* **2000**, *122*, 9500−9510.
(12) Reinhardt, B. A.; Brott, L. L.; Clarson, S. J.; Dillard, A. G.; Bhatt, J. C.; Kannan, R.; Yuan, L.; He, G. S.; Prasad, P. N. *Chem. Mater.* **1998**, *10*, 1863−1874.

branched,[21] and dendrimer structures,[22,23] and organometallic complexes.[24,25] We have shown in previous work that the magnitude of δ for quasi-linear quadrupolar molecules depends on the degree of intramolecular charge transfer upon excitation, and that it is possible to increase dramatically the two-photon response by adding donor and acceptor groups to the conjugated backbone of the molecule.[10,11,26] To date, there has been relatively little work on functionalizing such two-photon chromophores to impart specific photochemical or photophysical properties.[27−29]

Measuring the concentration of ions and imaging their spatial distribution in biological systems at rest and with stimuli is of great interest for understanding physiological responses, such as signal transduction. Magnesium ions (Mg^{2+}) are important in mediating enzymatic reactions[30] and calcium acts as a universal second messenger in cells.[31] A large number of molecular sensors and detection schemes for these and other ions or small molecules have been developed.[32−38] If a molecule exhibits changes in linear or two-photon optical properties (absorption cross section, absorption/emission wavelengths, quantum yield, lifetime, etc.) in the presence of an analyte, then it may have utility in sensing schemes based on fluorescence detection, such as TPLSM.

A few studies have been performed on the two-photon absorption properties of ion responsive molecules. The chro-

mophores calcium orange, calcium green-1, and calcium crimson[39] exhibit different fluorescence intensities in the bound and unbound state; the fluorescence in the unbound form is quenched due to photoinduced intramolecular electron transfer.[32] These molecules have the largest reported two-photon action cross sections ($\eta\delta$, where η is the fluorescence quantum yield) for ion sensing molecules with values in the range of $1-30$ GM in the unbound form in the $800-900$ nm spectral region. Upon binding of calcium ions, $\eta\delta$, to which the two-photon induced fluorescence signal is proportional, increases to $50-100$ GM for these three molecules.[40] The addition of calcium ions does not change the shape of the spectra, and the authors state that the ratio of the fluorescence intensity between the bound and free forms is the same for one- and two-photon excitation. This suggests that the observed changes in $\eta\delta$ upon ion binding are due primarily to changes in the fluorescence quantum yield between the bound and unbound forms, for these molecules. For indo-1, a widely used probe for intracellular calcium measurements via ratiometric detection, the value of $\eta\delta$ at 700 nm was measured to be ∼4.5 GM in the low calcium regime, and ∼1.2 GM in the high calcium case.[41] Taking into account the variations of the fluorescence quantum yield (assuming that η is the same for one- and two-photon excitation), one would infer that $\delta = 12$ GM in the unbound form and is reduced to 2.1 GM in the high calcium regime. This indicates that δ can be modified by the binding of calcium ions for this dye. Another dye, fura-2, exhibits changes in the shape of the two-photon action spectrum. At ∼775 nm, the signal in the presence of calcium is ∼20 times less than that of the free species, whereas at 700 nm, $\eta\delta$ is the same for the bound and unbound species (∼10 GM).[40] Although the ion responsive compounds discussed above exhibit sizable contrast in the two-photon action upon binding, the magnitude of the two-photon absorption cross section and the $\eta\delta$ values are rather small.

We have pursued a design strategy for fluorescent ion responsive molecules with enhanced two-photon properties based on the covalent linkage of quasi-linear quadrupolar two-photon chromophores, that can provide large two-photon cross sections, to ligands capable of metal ion binding, wherein the terminal electron donors of the chromophore are also active participants in the ion-binding functionality. Specifically, we have investigated molecules in which one or two monoaza-15-crown-5-ether macrocyclic ligands are attached to a D−A−D two-photon chromophore (Figure 1) in such a way that nitrogen atoms of the crown groups act as electron donors for the conjugated system and take part in the ion binding. The reduction in electron donor strength upon binding can affect the symmetry and the degree of intramolecular charge transfer within the chromophore and potentially lead to significant changes in the strength and position of the two-photon absorption bands.

Crown ethers are well-known to bind alkali and alkaline earth metal ions, as well as other cations. Generally, the binding is not selective for a specific ion, but various cations can be complexed by the macrocycle and the association constant of the complex depends on factors such as the diameter of the

(13) Ventelon, L.; Moreaux, L.; Mertz, J.; Blanchard-Desce, M. *Chem. Commun.* **1999**, 2055−2056.
(14) Zojer, E.; Beljonne, D.; Kogej, T.; Vogel, H.; Marder, S. R.; Perry, J. W.; Brédas, J. L. *J. Chem. Phys.* **2002**, *116*, 3646−3658.
(15) Morel, Y.; Irimia, A.; Najechalski, P.; Kervella, Y.; Stephan, O.; Baldeck, P. L.; Andraud, C. *J. Chem. Phys.* **2001**, *114*, 5391−5396.
(16) Najechalski, P.; Morel, Y.; Stéphan, O.; Baldeck, P. L. *Chem. Phys. Lett.* **2001**, *343*, 44−48.
(17) Delysse, S.; Raimond, P.; Nunzi, J.-M. *Chem. Phys.* **1997**, *219*, 341−351.
(18) Belfield, K. D.; Hagan, D. J.; Van Stryland, E. W.; Schafer, K. J.; Negres, R. A. *Org. Lett.* **1999**, *1*, 1575−1578.
(19) Cho, B. R.; Son, K. H.; Lee, S. H.; Song, Y.-S.; Lee, Y.-K.; Jeon, S.-J.; Choi, J. H.; Lee, H.; Cho, M. *J. Am. Chem. Soc.* **2001**, *123*, 10 039−10 045.
(20) Beljonne, D.; Wenseleers, W.; Zojer, E.; Shuai, Z.; Vogel, H.; Pond, S. J. K.; Perry, J. W.; Marder, S. R.; Brédas, J.-L. *Adv. Funct. Mater.* **2002**, *12*, 631−641.
(21) Chung, S.-J.; Kim, K.-S.; Lin, T.-C.; He, G. S.; Swiatkiewicz, J.; Prasad, P. N. *J. Phys. Chem. B* **1999**, *103*, 10 741−10 745.
(22) Drobizhev, M.; Karotki, A.; Rebane, A.; Spangler, C. W. *Opt. Lett.* **2001**, *26*, 1081−1083.
(23) Adronov, A.; Frechet, J. M. J. *Chem. Mater.* **2000**, *12*, 2838−2841.
(24) McDonagh, A. M.; Humphrey, M. G.; Samoc, M.; Luther-Davies, B. *Organometallics* **1999**, *18*, 5195−5197.
(25) Hurst, S. K.; Humphrey, M. G.; Isoshima, T.; Wostyn, K.; Asselberghs, I.; Clays, K.; Persoons, A.; Samoc, M.; Luther-Davies, B. *Organometallics* **2002**, *21*, 2024−2026.
(26) Pond, S. J. K.; Rumi, M.; Levin, M. D.; Parker, T. C.; Beljonne, D.; Day, M. W.; Brédas, J.-L.; Marder, S. R.; Perry, J. W. *J. Phys. Chem. A* **2002**, *106*, 11 470−11 480.
(27) Zhou, W.; Kuebler, S. M.; Braun, K. L.; Yu, T.; Cammack, J. K.; Ober, C. K.; Perry, J. W.; Marder, S. R. *Science* **2002**, *296*, 1106−1109.
(28) Frederiksen, P. K.; Jørgensen, M.; Ogilby, P. R. *J. Am. Chem. Soc.* **2001**, *123*, 1215−1221.
(29) Poulsen, T. D.; Frederiksen, P. K.; Jørgensen, M.; Mikkelsen, K. V.; Ogilby, P. R. *J. Phys. Chem. A* **2001**, *105*, 11 488−11 495.
(30) Suzuki, Y.; Komatsu, H.; Ikeda, T.; Saito, N.; Araki, S.; Citterio, D.; Hisamoto, H.; Kitamura, Y.; Kubota, T.; Nakagawa, J.; Oka, K.; Suzuki, K. *Anal. Chem.* **2002**, *74*, 1423−1428.
(31) Takahashi, A.; Camacho, P.; Lechleiter, J. D.; Herman, B. *Physiol. Rev.* **1999**, *79*, 1089−1125.
(32) Valeur, B. *Molecular Fluorescence: Principles and Applications*; Wiley: VCH: Weinheim, 2002.
(33) Lakowicz, J. R., Ed. *Probe Design and Chemical Sensing*; Plenum Press: New York, 1994; Vol. 4.
(34) McQuade, D. T.; Pullen, A. E.; Swager, T. M. *Chem. Rev.* **2000**, *100*, 2537−2574.
(35) Hancock, R. D.; Martell, A. E. *Chem. Rev.* **1989**, *89*, 1875−1914.
(36) de Silva, A. P.; Gunarante, H. Q. N.; Gunnlaugsson, T.; Huxley, A. J. M.; McCoy, C. P.; Rademacher, J. T.; Rice, T. E. *Chem. Rev.* **1997**, *97*, 1515−1566.
(37) An, H.; Bradshaw, J. S.; Izatt, R. M.; Yan, Z. *Chem. Rev.* **1994**, *94*, 939−991.
(38) Ikeda, A.; Shinkai, S. *Chem. Rev.* **1997**, *97*, 1713−1734.

(39) These chromophores are commercially available from Molecular Probes, Inc. (Eugene, OR).
(40) Xu, C.; Williams, R. M.; Zipfel, W.; Webb, W. W. *Bioimaging* **1996**, *4*, 198−207.
(41) Xu, C.; Webb, W. W. *J. Opt. Soc. Am. B* **1996**, *13*, 481−491.
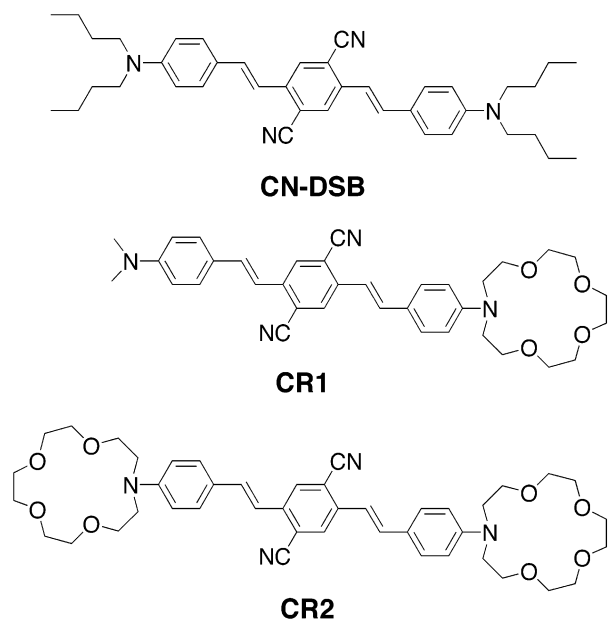
Figure 1. Molecular structures of the control compound (**CN−DSB**) and the mono-aza-crown-ether substituted chromophores (**CR1** and **CR2**).

ions relative to the size of the cavity formed by the macrocycle, the number of binding sites on the crown, the type of donor atoms (e.g., oxygen, nitrogen, or sulfur), and the solvent. Upon binding, the positive charge density of the metal ion can lead to a reduction in electron density on the coordinating aza nitrogen atom and thereby cause changes in the optical properties of the chromophore.[42−48]

In this paper, we report on the effects of magnesium ion binding on the linear and two-photon spectroscopic properties of mono- and bis-(aza-15-crown-5-ether) substituted D−A−D dyes. Following a description of the experimental and computational methods and synthetic details, we present results on (1) the one-photon electronic absorption properties, (2) the binding constants for Mg^{2+} ions and the absorption spectra for the bound species, (3) the fluorescence quantum yields and lifetimes of the free chromophores and bound species, (4) the two-photon fluorescence excitation spectra in the absence and presence of Mg^{2+}, (5) the predictions of quantum chemical calculations, which have been used to model the effect of ion binding on the strength and position of the lowest energy two-photon electronic absorption band, and (6) the estimation of sensitivity and contrast figures-of-merit for the crown substituted two-photon chromophores that have been examined. We discuss the modification of the one- and two-photon spectroscopic properties of the systems studied in terms of the change in the donating ability of the terminal amino substituents when the aza-nitrogen lone pair electrons are involved in ion binding.

(42) Fery-Forgues, S.; Le Bris, M.-T.; Guette, J.-P.; Valeur, B. *J. Phys. Chem.* **1988**, *92*, 6233−6237.
(43) Bourson, J.; Valeur, B. *J. Phys. Chem.* **1989**, *93*, 3871−3876.
(44) Rurack, K.; Rettig, W.; Resch-Genger, U. *Chem. Commun.* **2000**, 407−408.
(45) Bricks, J. L.; Slominskii, J. L.; Kudinova, M.; Tolmachev, A. I.; Rurack, K.; Resch-Genger, U.; Rettig, W. *J. Photochem. Photobiol. A* **2000**, *132*, 193−208.
(46) Das, S.; Thomas, K. G.; Thomas, K. J.; Kamat, P. V.; George, M. V. *J. Phys. Chem.* **1994**, *98*, 9291−9296.
(47) Marcotte, N.; Fery-Forgues, S.; Lavabre, D.; Marguet, S.; Pivovarenko, V. G. *J. Phys. Chem. A* **1999**, *103*, 3163−3170.
(48) Marcotte, N.; Plaza, P.; Lavabre, D.; Fery-Forgues, S.; Martin, M. M. *J. Phys. Chem. A* **2003**, *107*, 2394−2402.

Experimental Section

(i) Synthesis. ^{1}H NMR spectra were recorded on a Varian Unity Plus-500 NMR spectrometer using the residual proton resonance of the solvent as the internal standard. Chemical shifts are reported in parts per million (ppm). When peak multiplicities are given, the following abbreviations are used: s, singlet; d, doublet; t, triplet; m, multiplet. ^{13}C NMR spectra were recorded as proton decoupled spectra on a Varian Unity-300 using the carbon signal of the deuterated solvent as the internal standard. Elemental analyses were performed by Desert Analytics, Tucson, AZ. All solvents and reagents were used as obtained from commercial sources.

4-(Dimethylamino)benzaldehyde (**1**) was purchased from Aldrich and was used as received. 1,4-Bis(diethylphosphorylmethyl)-2,5-dicyanobenzene (**2**),[49] 4-(1-aza-4,7,10,13-tetraoxacyclopentadecyl)-benzaldehyde (**3**),[50] and 2,5-dicyano-1,4-bis[2-(4-(di-*n*-butylamino)phenyl)-vinyl]benzene (**CN−DSB**)[26] were synthesized according to literature procedures.

[2,5-Dicyano-4-[2-(4-dimethylaminophenyl)vinyl]benzyl]-phosphonic Acid Diethyl Ester (4). Aldehyde **1** (170 mg, 1.14 mmol), and diphosphonate **2** (500 mg, 1.17 mmol) were dissolved in 10 mL of tetrahydrofuran (THF), and the solution was cooled to 0 °C. To this solution, 530 mg (4.72 mmol) of potassium *tert*-butoxide in 10 mL of THF was added dropwise, and the reaction mixture was stirred for 3 h at 0 °C. Water was added to the reaction mixture, and the product was extracted with ethyl acetate. The organic layer was dried with $MgSO_4$ followed by evaporation of the solvent. The crude product was separated by column chromatography with a gradient of hexane in dichloromethane (20−0%) and ethyl acetate in dichloromethane (0−20%) and was used directly in the next step of the synthesis without further characterization.

2,5-Dicyano-1-[2-(4-dimethylaminophenyl)vinyl]-4-[2-[4-(1-aza-4,7,10,13-tetraoxacyclopentadecyl)phenyl]vinyl]benzene (CR1). Monophosphonate **4** (210 mg, 0.50 mmol) and aldehyde **3** (200 mg, 0.62 mmol) were dissolved in 10 mL of THF, and the solution was cooled to 0 °C. With stirring, a solution of potassium *tert*-butoxide (280 mg, 2.50 mmol) in 10 mL of THF was added to the solution slowly. After 1 h stirring at 0 °C, the reaction mixture was warmed to room temperature and stirred for 1 h. The reaction was quenched by water, and the product was extracted with dichloromethane. After drying with $MgSO_4$, the solvent was removed and the crude product was purified by column chromatography with a gradient of ethyl acetate in dichloromethane (0−20%). Yield 154 mg (0.26 mmol, 52%). The resulting solid was recrystallized from acetone to give red needles. ^{1}H NMR (500 MHz, CDCl3) δ: 7.96 (s, 2H), 7.48 (d, *J* = 9 Hz, 2H), 7.45 (d, *J* = 9 Hz, 2H), 7.21 (d, *J* = 17 Hz, 1H), 7.20 (d, *J* = 16 Hz, 1H), 7.14 (d, *J* = 17 Hz, 1H), 7.12 (d, *J* = 16 Hz, 1H), 6.72 (d, *J* = 9 Hz, 2H), 6.68 (d, *J* = 9 Hz, 2H), 3.78 (t, *J* = 7 Hz, 4H), 3.67 (m, 16H), 3.03 (s, 6H). ^{13}C NMR (75 MHz, CDCl3) δ: 151.2, 148.7, 138.7, 138.7, 134.6, 134.5, 129.1, 129.1, 128.9, 123.8, 123.6, 117.3, 117.1, 117.0, 114.2, 114.2, 112.2, 111.7, 71.5, 70.4, 70.2, 68.5, 52.8, 40.4. Anal. Calcd for $C_{36}H_{40}N_4O_4$: C, 72.95; H, 6.80; N, 9.45; O, 10.80. Found: C, 72.89; H, 6.96; N 9.50; O, 10.65.

2,5-Dicyano-1,4-bis[2-(4-(1-aza-4,7,10,13-tetraoxacyclopentadecyl)phenyl)vinyl]benzene (CR2). Aldehyde **3** (500 mg, 1.55 mmol) and diphosphonate **2** (322 mg, 0.75 mmol) were dissolved in 10 mL of THF, and the solution was cooled to 0 °C. Potassium *tert*-butoxide (560 mg, 5.0 mmol) in 10 mL of THF was added to the solution slowly. After the mixture was stirred for 3 h at 0 °C, 100 mL of water was added, and a red powder precipitated. The powder was collected, washed with water, and dried under vacuum. Yield 300 mg (0.39 mmol, 52%). The solid was recrystallized from dichloromethane to give a red

(49) Wenseleers, W.; Stellacci, F.; Meyer-Friedrichsen, T.; Mangel, T.; Bauer, C. A.; Pond, S. J. K.; Marder, S. R.; Perry, J. W. *J. Phys. Chem. B* **2002**, *106*, 6853−6863.
(50) Dix, J. P.; Vogtle, F. *Chem. Ber.* **1980**, *113*, 457−470.

powder. ^{1}H NMR (500 MHz, CDCl$_3$) δ: 7.95 (s, 2H), 7.45 (d, $J = 9$ Hz, 4H), 7.19 (d, $J = 16$ Hz, 2H), 7.12 (d, $J = 16$ Hz, 2H), 6.68 (d, $J = 9$ Hz, 4H), 3.78 (t, $J = 7$ Hz, 8H), 3.67 (m, 32H). ^{13}C NMR (75 MHz, CDCl$_3$) δ: 148.6, 138.6, 134.5, 130.0, 129.0, 123.5, 117.3, 116.9, 114.1, 111.7, 71.4, 70.3, 70.2, 68.5, 52.8. Anal. Calcd for C$_{44}$H$_{54}$N$_4$-O$_8$: C, 68.91; H, 7.10; N, 7.31; O, 16.69. Found: C, 69.03; H, 7.18; N 7.46; O, 16.33.

(ii) Spectroscopic Measurements. All solutions were prepared in spectrophotometric grade acetonitrile (Aldrich). Magnesium perchlorate (ACS reagent grade, Aldrich), tetra-*n*-butylammonium bromide (Fluka), and concentrated hydrochloric acid (EM Science) were used as received. All solutions were allowed to equilibrate for at least 1 h in the dark prior to optical measurements.

Absorption spectra were obtained on a Hewlett-Packard 8453 diode array spectrophotometer. The peak molar extinction coefficient, ϵ_{max}, for the chromophores studied was obtained from a linear regression analysis of absorbance versus dye concentration using the Beer–Lambert equation. Dilutions of two independent stock solutions of the unbound chromophores allowed to investigate concentrations spanning a range of nearly 2 orders of magnitude and absorption spectra were obtained in 0.1 or 1 cm path length cuvettes, as needed. No deviations from the Beer–Lambert law were observed at the concentrations that were used in the measurements of the two-photon spectra, indicating the absence of aggregation. To measure the extinction coefficients of the complexes, spectra were collected in 1 and 10 cm path length cuvettes for several independent solutions (serial dilutions of the sample were not appropriate as this would have perturbed the equilibrium). The uncertainty in ϵ_{max} is < 5%.

A Spex Fluorolog-2 spectrofluorimeter was used for the measurement of the fluorescence spectra. All spectra have been corrected by subtraction of the spectrum of a solvent blank sample and by introduction of the instrument correction factor, which accounts for the wavelength dependence of the instrument response function as well as for variations in excitation lamp power. The dye concentration (typically 1×10^{-7} M) for steady-state fluorescence experiments was kept as low as possible in order to minimize reabsorption effects. The fluorescence quantum yield, η, was determined using 9,10-bis(phenylethynyl)anthracene (BPEA) in cyclohexane ($\eta = 1.0$)[51] as a reference compound, and under the following conditions: [Mg^{2+}] $\sim$ 30 mM, [^{n}Bu$_4$N$^+$] = 35 mM, [HCl] = 39 mM, and excitation wavelength = 400 nm. The absorbance of the solutions for fluorescence quantum yield measurements was less than 0.02 at the excitation wavelength, so that attenuation of the excitation beam in the sample was small. The experimental uncertainty in η is 10%.

Fluorescence lifetimes were measured using the time-correlated single photon counting technique.[52] The molecules were excited at 305 nm using the frequency-doubled output of a picosecond-pulse dye laser and the fluorescence was detected perpendicular to the excitation beam after passing through an analyzing polarizer set at the magic angle and a monochromator. The details of the experimental setup and method of analysis of the data have been described previously.[53] The instrumental response function was $\sim$90 ps (full width at half-maximum). The experimental conditions used were the following: [dye] $\sim$ 1 $\times$ 10^{-6} M, [Mg^{2+}] = 17 mM, [^{n}Bu$_4$N$^+$] = 17 mM, [HCl] = 40 mM. The fluorescence decays for **CN–DSB** and **CR1** were collected at 650 nm, those for **CR2** at 640 nm. The χ^2 values for the fits of the fluorescence decays were all between 1.06 and 1.21. The uncertainty in τ is 1–5% for the monoexponential decays, and 5–10% for the multiexponential decays.

Two-photon excitation spectra were measured using the two-photon induced fluorescence technique[41] using a Ti:Sapphire laser excitation

source (Tsunami, Spectra-Physics). This laser generates $\sim$85 fs pulses at a repetition rate of 82 MHz in the wavelength range of 710–1000 nm. The optical set up has been described previously.[49] Coumarin 307 in methanol and fluorescein in pH 11 water, both of which have been well characterized in the literature,[41] were used as reference (*r*) compounds. The two-photon absorption cross section of a sample compound (*s*) can be calculated at each wavelength according to

$$\delta_s = \frac{S_s \eta_r \Phi_r C_r}{S_r \eta_s \Phi_s C_s} \delta_r \qquad (1)$$

where S is the detected two-photon induced fluorescence signal, η is the fluorescence quantum yield, and C is the concentration of the chromophore. Φ is the collection efficiency of the experimental setup and accounts for the wavelength dependence of the detectors and optics as well as the difference in refractive indexes between the solvents in which the reference and sample compounds are dissolved.[11] The concentration of the solutions were in the range of 1×10^{-6} to 1×10^{-5} M. The fluorescence detection was performed at the same wavelength for reference and sample compounds (both 625 and 600 nm detection wavelengths were used). The output signal was averaged for 60 s. The measurements were conducted in an intensity regime where the fluorescence signal showed a quadratic dependence on the intensity of the excitation beam. The uncertainty in the measured cross sections is about 15%.

(iii) Binding Constant Determination. The binding constants for the complexes between the **CR1** or **CR2** chromophores and magnesium ions were determined by spectrophotometric titration. The concentration of Mg^{2+} was in the range 5×10^{-7} to 2×10^{-2} M. The chromophore concentration was 1.02×10^{-5} M.

Modeling and Computational Methods

(i) Analysis of the Complexation Equilibria. The equilibrium expression for the formation of a 1:1 dye:metal complex is as follows

$$D + M \overset{K_1}{\rightleftharpoons} DM \qquad (2)$$

where D is the dye, M is the metal ion, DM is the complex, and K_1 is the binding constant. K_1 can be determined from measurements of absorbance as a function of ion concentration using the following equation[54]

$$\frac{\Delta A}{L} = \frac{[D_t]K_1 \Delta\epsilon_{11}[M]}{1 + K_1[M]} \qquad (3)$$

In eq 3, ΔA is the difference in absorbance at a particular wavelength between the pure dye solution and the solution of dye and metal ion ($A_0 - A$), L is the path length, $[D_t]$ is the total dye concentration, $[M]$ is the concentration of the free metal, and $\Delta\epsilon_{11}$ is the change in extinction coefficient at the measurement wavelength between the dye and the dye:metal complex ($\epsilon_D - \epsilon_{DM}$). Equation 3 is valid if the free metal ion concentration is not significantly altered by binding.

In the case where the chromophore can form 1:1 (**CR2**:Mg^{2+}) and 1:2 (**CR2**:2Mg^{2+}) complexes, the system is described by the following equilibria

$$D + M \overset{K_{11}}{\rightleftharpoons} DM \qquad (4)$$

$$DM + M \overset{K_{12}}{\rightleftharpoons} DM_2 \qquad (5)$$

It can be shown[54] that the change in absorbance (ΔA) at a specified wavelength is given by

(51) Berlman, I. B. *Handbook of Fluorescence Spectra of Aromatic Molecules*, 2nd ed.; Academic Press: New York, 1971.
(52) O'Connor, D. V.; Phillips, D. *Time-Correlated Single Photon Counting*; Academic Press: London, 1984.
(53) Khundkar, L. R.; Perry, J. W.; Hanson, J. E.; Dervan, P. B. *J. Am. Chem. Soc.* **1994**, *116*, 9700–9709.

(54) Connors, K. A. *Binding Constants: The Measurement of Molecular Complex Stability*; John Wiley and Sons: New York, 1987.

$$\frac{\Delta A}{L} = \frac{[D_t](K_{11}\Delta\epsilon_{11}[M] + K_{11}K_{12}\Delta\epsilon_{12}[M]^2)}{1 + K_{11}[M] + K_{11}K_{12}[M]^2} \quad (6)$$

where K_{11} and K_{12} are the two binding constants, as described in eqs 4 and 5, $\Delta\epsilon_{12} = (\epsilon_D - \epsilon_{DM2})$, and the other parameters have the same meaning as in eq 3. This treatment is again valid under the condition that the metal ion concentration is unchanged by the binding.

(ii) Determination of Transition Dipole Moments. We have previously shown[10,11,14] that the two-photon properties of linear quadrupolar conjugated molecules, substituted with electron accepting and withdrawing groups, can be described reasonably well by a simple model that includes three electronic states: the ground state (g), the lowest excited state (e), and a higher lying two-photon state (e'). According to this model, the two-photon absorption cross section depends on the transition dipole moments (M) between states g and e, and between states e and e', and on the energies (E) of the three states. Specifically, at the two-photon resonance ($2\hbar\omega = E_{ge'}$), the peak two-photon cross section is given by

$$\delta_{max} \approx \frac{16\pi^2 L^4 \hbar\omega^2}{5n^2c^2}\frac{M_{ge}^2 M_{ee'}^2}{(E_{ge} - E_{ge'}/2)^2\Gamma_{ge'}} \quad (7)$$

where $\hbar = h/2\pi$, h is Planck's constant, c is the speed of light, n is the refractive index of the medium, ω is the excitation frequency, L is the Lorentz local field factor ($L = (n^2 + 2)/3$), and $\Gamma_{ge'}$ represents the overall bandwidth (full width at half-maximum) associated with the $g{\to}e'$ transition. Equation 7 is written in the cgs system of units.

After determining the transition moment M_{ge} from the integrated molar extinction coefficient for the $g{\to}e$ transition,[55,56] the state energies from the peak in the one- and two-photon spectra, and assuming $\Gamma_{ge'} \approx 0.1$ eV (a value consistent with the bandwidth of the two-photon spectra for many quadrupolar chromophores),[11] the excited-state transition moment $M_{ee'}$ can be estimated, based on experimental data, via the following equation

$$M_{ee'} = \frac{nc(E_{ge} - \hbar\omega)}{4\pi\omega L^2 M_{ge}}\left(\frac{5\Gamma_{ge'}\cdot\delta_{max}}{\hbar}\right)^{1/2} \quad (8)$$

(for acetonitrile $n = 1.3442$).

(iii) Quantum Chemical Calculations. The molecular geometries were optimized at the B3LYP/6-31G* level[57] in the density functional theory (DFT) formalism.[58,59] The geometries obtained with the semiempirical AM1 Hamiltonian utilized in several previous studies were significantly different from the DFT results for **CR2**:2Mg^{2+} and they appeared to be chemically unreasonable. This is most likely due to an improper description of the interaction of Mg^{2+} with the aza-crown ether. The transition energies and dipole moments of the compounds were then calculated by using the semiempirical INDO Hamiltonian[60,61] coupled to a multireference determinant single and double configuration-interaction (MRD-CI)[62] scheme in order to include electron correlations, which are especially important for the description of the TPA active states.[63–65] To describe the Coulomb repulsion terms, the Mataga–

(55) Birge, R. R. In *Ultrasensitive Laser Spectroscopy*; Kliger, D. S., Ed.; Academic Press: New York, 1983; pp 109–174.
(56) Herzberg, G. *Molecular Spectra and Molecular Structure. I. Spectra of Diatomic Molecules*, 2nd ed.; Van Nostrand Reinhold Company: New York, 1950.
(57) Becke, A. D. *J. Chem. Phys.* **1993**, *98*, 5648–5652.
(58) Koch, W.; Holthausen, M. C. *A Chemist's Guide to Density Functional Theory*; Wiley & Sons: New York, 2000.
(59) Parr, R. G.; Yang, W. *Density Functional Theory of Atoms and Molecules*; Oxford University Press: Oxford, 1989.
(60) Ridley, J.; Zerner, M. *Theor. Chim. Acta* **1973**, *32*, 111–134.
(61) Zerner, M. C.; Loew, G. H.; Kirchner, R. F.; Mueller-Westerhoff, U. T. *J. Am. Chem. Soc.* **1980**, *102*, 589–599.
(62) Buenker, R. J.; Peyerimhoff, S. D. *Theor. Chim. Acta* **1974**, *35*, 33–58.
(63) Tavan, P.; Schulten, K. *J. Chem. Phys.* **1986**, *85*, 6602–6609.
(64) Pierce, B. M. *J. Chem. Phys.* **1989**, *91*, 791–811.

Nishimoto (MN) potential[66] was used, as it has been found that this potential yields a better agreement with experimental spectroscopic data,[20,67] than the Ohno–Klopman (OK) potential[68,69] used previously.[10] The five determinants chosen as reference determinants in the MRD-CI procedure are those that dominate the description of the ground state, the lowest excited state, and the two-photon excited state. Specifically, these are: the self-consistent field determinant, the singly excited determinants with an electron excited from the HOMO to the LUMO, from the HOMO to the LUMO + 1, and from the HOMO − 1 to the LUMO, and the doubly excited determinant with both electrons excited from the HOMO to the LUMO (where HOMO is the highest occupied molecular orbital and LUMO is the lowest unoccupied molecular orbital). The active space included the highest 26 occupied and lowest 26 unoccupied orbitals for single excitations, and the highest 6 occupied and lowest 6 unoccupied orbitals for multiple excitations. The calculations were performed on isolated molecules in the vacuum ($n = 1$). The values of Im γ ($-\omega;\omega,-\omega,\omega$), which can be related to δ, were computed by using the perturbative Sum-over-State (SOS) expression[70] including the 300 lowest-lying singlet excited states.

Results

(i) Synthesis. Two molecules bearing one or two mono-aza-15-crown-5-ether macrocycles attached to a two-photon D−A−D chromophore have been synthesized and characterized. The synthetic scheme for the preparation of **CR1** and **CR2** is illustrated in Figure 2. The **CR1** chromophore has a donor−acceptor−donor structure with a distyrylbenzene π-backbone, and one of the donors is a dimethylamino group whereas the other is a mono-aza-15-crown-5-ether. The **CR2** chromophore is symmetrically substituted with two of the aza-crown ether moieties, one at each end. **CR1** and **CR2** were synthesized using Horner−Emmons coupling. The bis-crown chromophore **CR2** was obtained by reacting 2 equiv of the mono-crown ether benzaldehyde, **3**, with a dicyanobenzene bis-phosphonate precursor, **2**. To obtain the mono-aza crown chromophore **CR1**, 1 equiv of 4-(dimethylamino)benzaldehyde, **1**, was reacted with **2** to produce the mono-phosphonate intermediate, **4**, which was then reacted with the mono-crown aldehyde **3**. Also shown in Figure 1 is a dye based on a donor−acceptor−donor substituted distyrylbenzene (**CN−DSB**), which was previously studied in our laboratory and shown to possess a large two-photon absorption cross section ($\delta = 1750$ GM at 830 nm, in toluene).[26] **CN−DSB** lacks an ion binding functionality and was used for control experiments.

(ii) One-Photon Electronic Absorption Properties. The dye containing no crown ether groups (**CN−DSB**) exhibits an absorption maximum ($\lambda_{abs}^{(1)}$) at 482 nm in acetonitrile and has an ϵ_{max} of 7.6×10^4 M^{-1} cm^{-1} (see Figure 3 and Table 1). Substitution of a mono-aza-15-crown-5-ether group for one or two of the dialkylamino donor groups leads to a slight blue shift in the absorption spectra of **CR1** and **CR2** ($\lambda_{abs}^{(1)} = 468$ and 472 nm, respectively), suggesting that the aza-crown ether group is a slightly weaker donor group than the di-n-butylamino group. The peak extinction coefficients for the macrocycle containing chromophores are slightly lower than for the unsub-

(65) Shuai, Z.; Beljonne, D.; Brédas, J.-L. *J. Chem. Phys.* **1992**, *97*, 1132–1137.
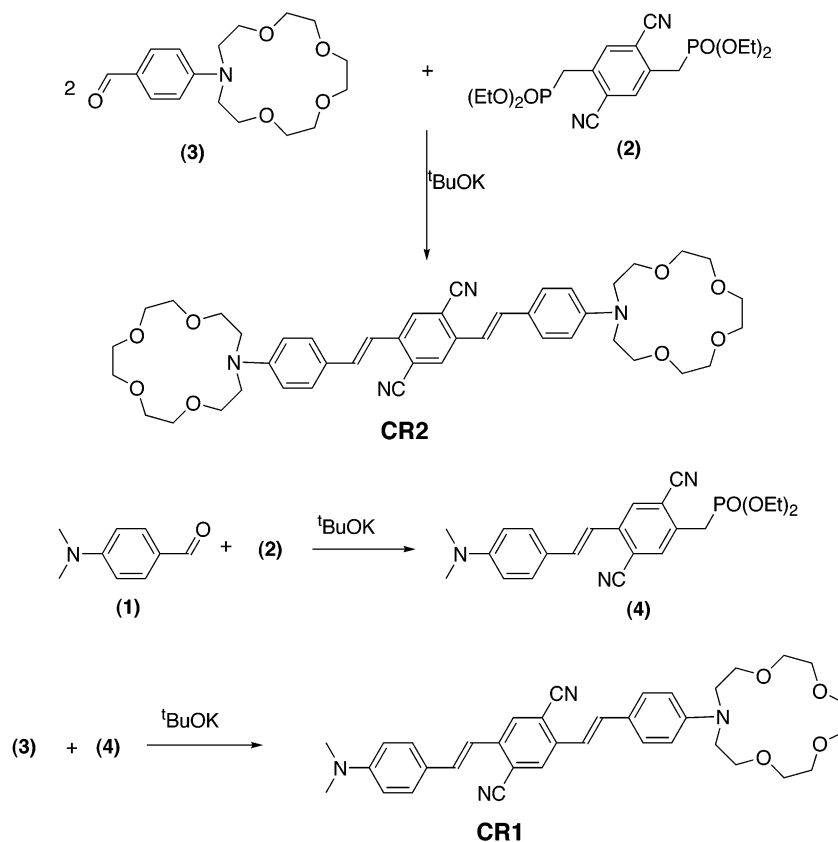(66) Mataga, N.; Nishimoto, K. *Z. Phys. Chem.* **1957**, *13*, 140–157.
(67) Zojer, E.; Wenseleers, W.; Pacher, P.; Barlow, S.; Halik, M.; Grasso, C.; Perry, J. W.; Marder, S. R.; Brédas, J.-L. *J. Phys. Chem. B* **2004**, *108*, 8641–8646.
(68) Ohno, K. *Theor. Chim. Acta* **1964**, *2*, 219–227.
(69) Klopman, G. *J. Am. Chem. Soc.* **1964**, *86*, 4550–4557.
(70) Orr, B. J.; Ward, J. F. *Mol. Phys.* **1971**, *20*, 513–526.

Figure 2. Synthetic scheme for the mono-crown (**CR1**) and bis-crown (**CR2**) compounds studied in this work.

stituted molecule ($\epsilon_{max} = 6.8 \times 10^4$ and 7.2×10^4 M^{-1} cm^{-1} for **CR1** and **CR2**, respectively). The transition dipole moment from the ground state (g) to the first excited state (e), M_{ge} is similar for **CN−DSB** and **CR1** (11 D) but somewhat smaller for **CR2** (9.6 D).[71]

The addition of magnesium ions to solutions of **CN−DSB** (Figure 3a) results in a small decrease in ϵ_{max} to 7.3×10^4 M^{-1} cm^{-1} at high Mg^{2+} concentration, but there is essentially no change in the shape or position of the band. On the contrary, the addition of magnesium ions to solutions of the crown-containing chromophores strongly affects their absorption spectra. The lowest energy absorption band of **CR1** undergoes a hypsochromic shift to 445 nm (see Figure 3b) and decreases in intensity to $\epsilon_{max} = 4.6 \times 10^4$ M^{-1} cm^{-1} for [Mg^{2+}] = 30 mM (as will be described in the following section, at this concentration ∼99% of the dye is present in the complexed form, **CR1**:Mg^{2+}). A new peak appears at higher energy (338 nm) and intensifies as the magnesium ion concentration is increased, reaching an ϵ_{max} of 2.5×10^4 M^{-1} cm^{-1} at high magnesium concentrations. An isosbestic point is observed at ∼430 nm and is consistent with the presence of an equilibrium between two absorbing species in solution. The effect of ion binding on the **CR2** chromophore is even more dramatic (Figure 3c). With two crown groups on the chromophore, it is possible for three species to be present in solution: the unbound **CR2**, a 1:1 (**CR2**:Mg^{2+}) complex, and a 1:2 (**CR2**:2Mg^{2+}) complex. At low magnesium concentrations (less than 0.1 mM), the absorption spectrum of the **CR2** solution is relatively similar

in shape to that of the **CR1**:Mg^{2+} complex, with a blue shift of the lowest energy band with respect to **CR2** and an additional peak at ∼340 nm. These features are indicative of the formation of the 1:1 **CR2**:Mg^{2+} complex. At higher ion concentrations (>5 mM), a peak at 378 nm due to the **CR2**:2Mg^{2+} complex becomes the dominant feature in the absorption spectrum, with an ϵ_{max} of 4.4×10^4 M^{-1} cm^{-1} for [Mg^{2+}] = 30 mM, at which concentration ∼89% of the dye is in the form of the **CR2**:2Mg^{2+} species (see below).

As a control experiment to test whether changes in ionic strength affect the optical properties of these chromophores, tetra-*n*-butylammonium cations (^{n}Bu$_4$N$^+$), which are too bulky to be complexed by the crown,[72,73] were added in high concentration (35 mM) to solutions of **CR1** and **CR2**. This did not significantly alter the strength or position of the linear absorption of **CR1** or **CR2** ($\epsilon_{max} = 6.7 \times 10^4$ and 7.0×10^4 M^{-1} cm^{-1}, respectively). Finally, to establish the role of the nitrogen donors in the features of the electronic spectra of the chromophores, absorption measurements were performed on **CR2** in acidic solution. Under strongly acidic conditions, both nitrogen atoms of **CR2** are expected to be protonated and, therefore, no longer serve as electron donors to the π-system. The absorption spectrum of **CR2** in the presence of 39 mM HCl in acetonitrile is shown in Figure 4. The absorption peak is at 362 nm and is ascribed to the **CR2**:2H$^+$ species. The ϵ_{max} is 4.8×10^4 M^{-1} cm^{-1}, which is similar to that of bis(*o*-methylstyryl)benzene.[51] The spectrum of the protonated **CR2** re-

(71) The transition moments were estimated for the lowest energy absorption band by a fitting procedure that accounts for a shoulder that is likely due to a higher energy electronic state, as described in ref 26.

(72) MacQueen, D. B.; Schanze, K. S. *J. Am. Chem. Soc.* **1991**, *113*, 6108−6110.
(73) Geue, J. P.; Head, N. J.; Ward, D.; Lincoln, S. F. *Dalton Trans.* **2003**, 521−526.
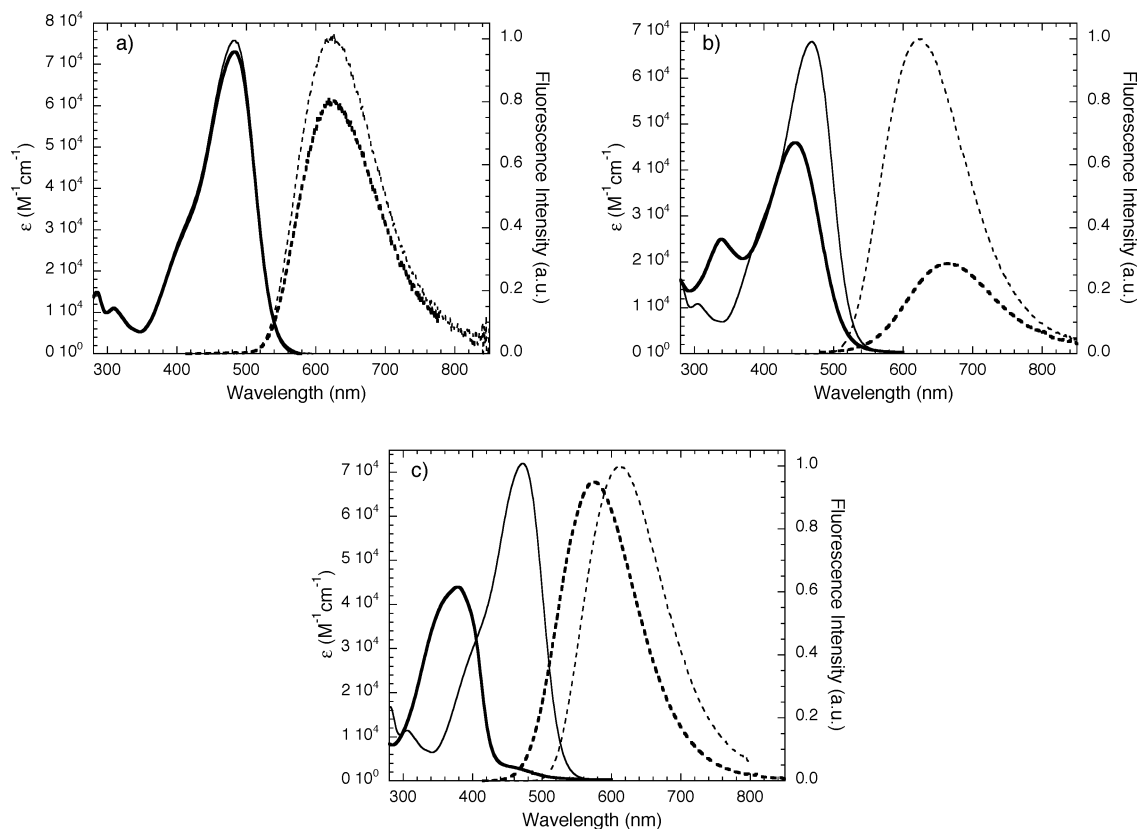
Figure 3. Linear electronic absorption and fluorescence emission spectra of (a) **CN−DSB**, (b) **CR1**, and (c) **CR2**. The thin solid line and thin dashed line are the absorption and fluorescence spectra of the dyes in acetonitrile. The thick solid and thick dashed lines are the absorption and emission spectra, respectively, of the dye-Mg^{2+} solution obtained using 10^{-7} M dye and 30 mM Mg^{2+}. For each molecule, the area of the fluorescence spectrum is proportional to the quantum yield.

Table 1. Linear Spectroscopic Data[a]

molecule/cation system	$\lambda_{abs}^{(1)}$ (nm)	ϵ_{max} (10^4 M^{-1} cm^{-1})	λ_{fl} (nm)	η	τ (ps)
CN−DSB	482	7.6	625	0.12	970
CN−DSB/Mg^{2+}	481	7.3	625	0.09	900
CR1	468	6.8	624	0.10	830
CR1/Mg^{2+}	445[b]	4.6[b]	665[b]	0.03[b]	1100
					420
CR1/$^nBu_4N^+$	468	6.7	626	0.12	820
CR2	472	7.2	610	0.20	1280
CR2/Mg^{2+}	378[c]	4.4[c]	576[c]	0.19[c]	1300
					2100
					730
CR2/$^nBu_4N^+$	472	7.0	610	0.23	1260
CR2/H^+	362	4.8	410	0.82	1440
					423

[a] Linear absorption maximum ($\lambda_{abs}^{(1)}$), molar peak extinction coefficient (ϵ_{max}), fluorescence emission maximum (λ_{fl}), fluorescence quantum yield (η), and fluorescence lifetime (τ). [b] Equilibrium percentage: **CR1**:Mg^{2+} = 99%, **CR1** = 1% (for the binding constant reported in the Results section, part *iii*). [c] Equilibrium percentage: **CR2**:$2Mg^{2+}$ = 89%, **CR2**:Mg^{2+} = 11%, **CR2** = 0.05% (for the binding constants reported in the Results section, part *iii*).

sembles that of **CR2** at high [Mg^{2+}], where a large fraction of the 1:2 complex is present. The similarity of the spectra of **CR2** in the protonated form and in the 1:2 complex with Mg^{2+} is consistent with the nitrogen lone pair not interacting significantly with the π-system upon ion binding. Such similarities in the absorption spectra of the ion-bound form of the aza-crown chromophores and the protonated dye[72] or a modified dye in which the crown is replaced by a hydrogen[42,43] have been observed for other aza-crown ether substituted systems.
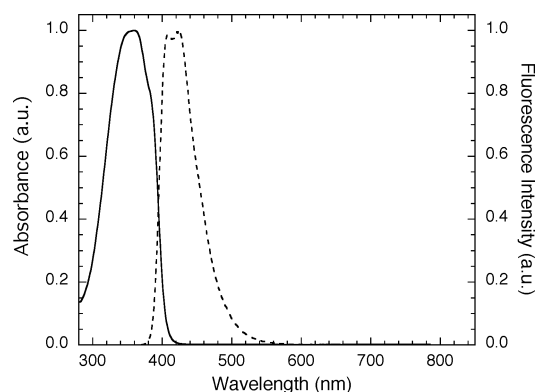
Figure 4. Linear absorption (solid line) and emission (dashed line) spectra of **CR2** in the presence of 39 mM HCl in acetonitrile.

(iii) Binding Constant Determination. To determine the distribution of species in the solutions in the presence of magnesium ions, the binding constants of **CR1** and **CR2** with Mg^{2+} were determined as described in the Experimental Section. Absorption spectra of **CR1** ($[D_t] \approx 1 \times 10^{-5}$ M) were collected for solutions containing Mg^{2+} in the concentration range of 5×10^{-7} M to 2×10^{-2} M (representative spectra are shown in Figure 5a). The change in absorption at 468 nm is shown in Figure 5b and can be fitted reasonably well by eq 3, consistent with a single-step complexation equilibrium. The parameters that give the best fit to the experimental data are $K_1 = 3500$ M^{-1} and $\Delta\epsilon_{11}(468 \text{ nm}) = 3.0 \times 10^4$ M^{-1} cm^{-1}, with an uncertainty of about 10%. A similar K_1 is obtained from the absorption data at 338 nm. The ϵ_{max} for the **CR1**:Mg^{2+} complex
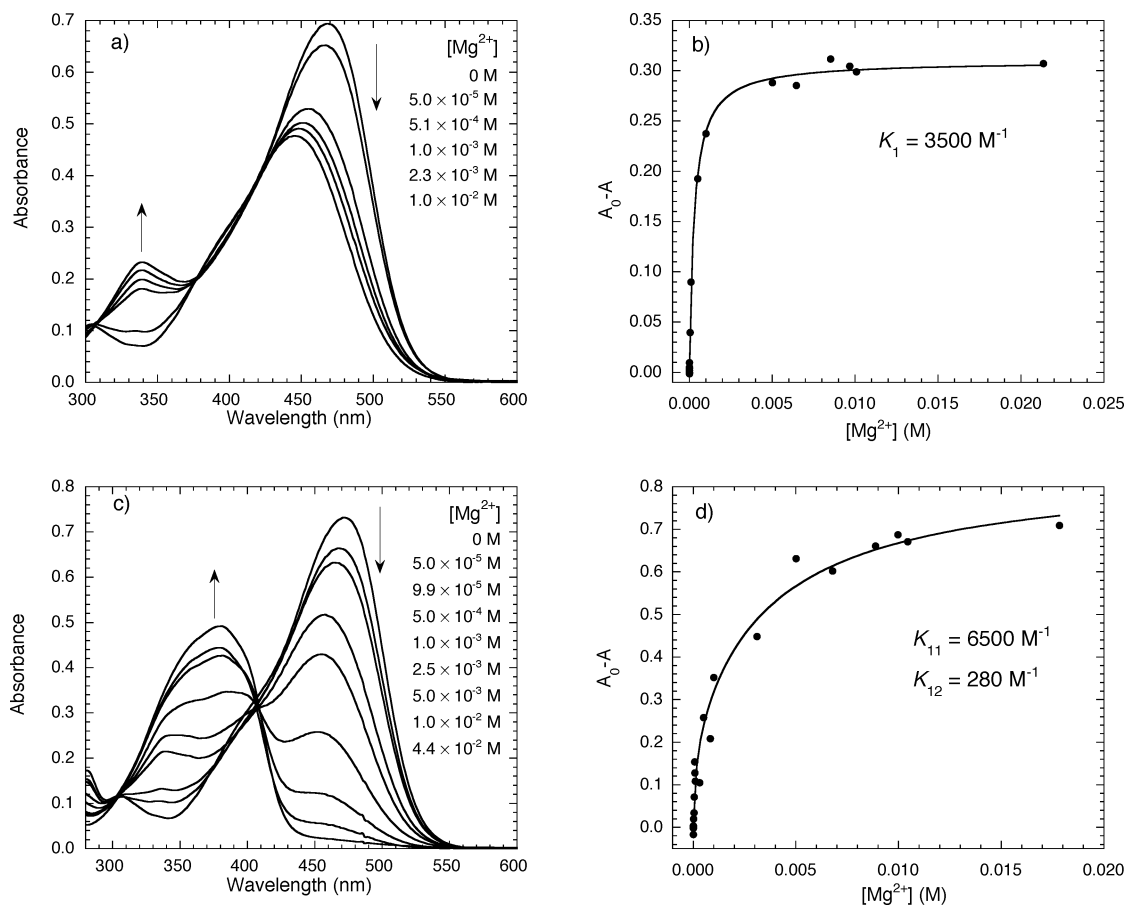
Figure 5. (a) Absorption spectrum of **CR1** as a function of [Mg²⁺]. Only spectra at selected concentrations are shown for clarity. The arrows indicate the trend for increasing [Mg²⁺]. The dye concentration is 1×10^{-5} M. (b) Change in absorbance at 468 nm as a function of [Mg²⁺] for **CR1**. The line is the best fit of the data to eq 3. (c) Absorption spectrum of **CR2** as a function of [Mg²⁺]. Only spectra at selected concentrations are shown for clarity. The arrows indicate the trend for increasing [Mg²⁺]. The dye concentration is 1×10^{-5} M. (d) Change in absorbance of **CR2** at 472 nm as a function of [Mg²⁺]. The line is the best fit of the data to eq 6.

can be estimated from $\Delta\epsilon_{11}$ and is consistent with the experimental value obtained at high [Mg²⁺].

For the **CR2** chromophore, the binding can be described well by a two-step complexation equilibrium (eqs 4 and 5). Representative absorption spectra of **CR2** with magnesium concentrations varying from 5×10^{-7} M to 2×10^{-2} M are shown in Figure 5c. Equation 6 was used to fit the experimental data at several wavelengths using a nonlinear least-squares method (see Figure 5d for data corresponding to $\lambda = 472$ nm). The fitting results are $K_{11} = 6500$ M⁻¹ and $K_{12} = 280$ M⁻¹, $\Delta\epsilon_{11}(472 \text{ nm}) = 2.4 \times 10^4$ M⁻¹ cm⁻¹, and $\Delta\epsilon_{12}(472 \text{ nm}) = 8.1 \times 10^4$ M⁻¹ cm⁻¹. The uncertainty is around 10% for K_{11}, and higher for K_{12} (20–30%). The extinction coefficients for the individual species that can be calculated from the fitting parameters are similar to those measured experimentally on solutions with a large excess of magnesium ions. Specifically, ϵ of the **CR2**:2Mg²⁺ complex at 340 nm is calculated to be 3.9×10^4 M⁻¹ cm⁻¹ from the fit. From an experimental spectrum with [Mg²⁺] $= 4.4 \times 10^{-2}$ M, a value of $\epsilon(340 \text{ nm}) = 3.5 \times 10^4$ M⁻¹ cm⁻¹ is obtained. At this concentration the fractions of the different species are estimated to be: < 0.03% **CR2** dye, 7.5% 1:1 complex, and 92.5% 1:2 complex using the binding constants obtained from the fit.

The fitting procedure described above is based on data obtained at particular wavelengths. To obtain absorption spectra of the individual species in solution and to make full use of all

the spectroscopic information collected for a given chromophore, a global fitting procedure for the full absorption spectra over a range of ion concentrations was implemented. The details of the fitting procedure are described in the Supporting Information. This fitting procedure resulted in a binding constant for **CR1** of $K_1 = 3530$ M⁻¹, a value which is in very good agreement with that obtained from the single wavelength fit (3500 M⁻¹). The binding constant for the formation of the **CR2**:Mg²⁺ complex is $K_{11} = 6060$ M⁻¹, again similar to the single wavelength value (6500 M⁻¹), and $K_{12} = 455$ M⁻¹ for the formation of **CR2**:2Mg²⁺. The two estimates for K_{12} (455 M⁻¹ from the global fitting, and 280 M⁻¹ from eq 6) are somewhat different, but they are within error bars of each other, for an uncertainty of 30%. The absorption spectra of the individual unbound and complexed species, as obtained from the global fitting procedure, are shown in Figure 6. The **CR1**:Mg²⁺ and **CR2**:Mg²⁺ spectra are very similar in position, shape, and intensity, suggesting a similar electronic structure for these two species. The **CR2**:2Mg²⁺ absorption spectrum resembles that observed for **CR2**:2H⁺, again supporting the interpretation that in the ground-state geometry the nitrogen donor groups are nearly completely decoupled from the π-system, when involved in ion binding.

(iv) Fluorescence Quantum Yields and Lifetimes. The fluorescence spectra of the three uncomplexed molecules (**CN⁻ DSB**, **CR1**, and **CR2**) in acetonitrile (Figure 3) are unstructured
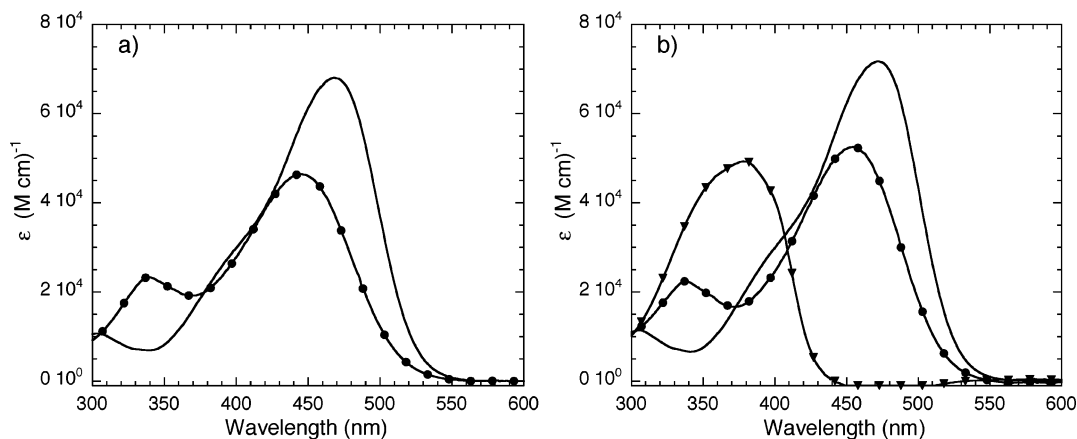
Figure 6. Absorption spectra of (a) **CR1** (solid line) and **CR1**:Mg^{2+} complex (circles), and (b) **CR2** (solid line), **CR2**:Mg^{2+} complex (circles) and **CR2**:2Mg^{2+} complex (triangles) obtained from a global fitting (see text for details).
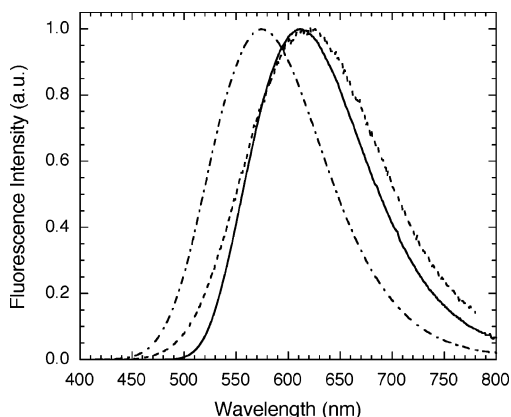

Figure 7. Fluorescence emission spectra of **CR2** with no magnesium (solid line), 2 mM Mg^{2+} (dotted line) and 30 mM Mg^{2+} (dot−dashed line). In all cases, the peak intensity has been normalized to one.

and have fluorescence maxima (λ_{fl}) located at 625 nm for **CN− DSB** and **CR1** and at 610 nm for **CR2**. These molecules exhibit large Stokes' shifts ($\nu_{abs}^{(1)} - \nu_{fl}$) of 4750 cm^{-1} for **CN−DSB**, 4790 cm^{-1} for **CR2**, and 5340 cm^{-1} for **CR1**. Their fluorescence quantum yields (η) in acetonitrile are in the range 0.10−0.20 in the absence of complexing metal ions (Table 1). **CN−DSB** shows a small decrease in quantum yield when 30 mM Mg^{2+} is added to the solution ($\eta = 0.09$ versus 0.12) but no shift in the position of the fluorescence band is observed (Figure 3a). The quantum yields of **CR1** and **CR2** in the presence of 35 mM ^{n}Bu$_4$N$^+$ are 0.12, and 0.23, respectively, which indicates that the effect of ionic strength on η is small. Moreover, the addition of ^{n}Bu$_4$N$^+$ does not produce any significant change in the shape and position of the fluorescence band. In contrast, the spectrum of **CR1** shows a 40 nm (0.12 eV) red shift on binding Mg^{2+}, and a reduced quantum yield of 0.03 is obtained under high Mg^{2+} concentration (30 mM) conditions. The Stokes' shift for **CR1** increases upon binding (7454 cm^{-1}), suggesting that the relaxation energy in the excited state is larger for the complex than for the unbound dye. The fluorescence of **CR2** shows a more complex behavior (Figure 7). At low magnesium concentrations (for 2 mM Mg^{2+} the fractions of the dye containing species are as follows:[74] 34% **CR2**:2Mg^{2+}, 61% **CR2**:Mg^{2+}, 5% free **CR2**) the fluorescence spectrum red shifts

---

(74) All the solution compositions that are reported from here on were calculated using the values of the binding constants shown in Figure 5b or 5d, as appropriate (single wavelength fitting).

by ∼10 nm (0.03 eV), broadens, and the effective quantum yield of the solution decreases ($\eta = 0.12$). This suggests that the **CR2**:Mg^{2+} species has fluorescence properties similar to those of **CR1**:Mg^{2+}. At higher magnesium concentrations (30 mM Mg^{2+}, for which the solution composition is 89% **CR2**:2Mg^{2+}, 11% **CR2**:Mg^{2+}, < 1% **CR2**), the fluorescence spectrum blue shifts by 35 nm (0.12 eV) compared to the unbound species, but the fluorescence quantum yield of this solution is similar to that of the unbound species ($\eta = 0.19$). In the presence of 30 mM Mg^{2+}, the Stokes' shift is 9090 cm^{-1}, nearly twice that of the unbound species. The excited-state relaxation energy is extremely large in the presence of ions, resulting in a fluorescence maximum which is somewhat similar to the free dye, whereas there is a larger difference in the absorption maxima (∼100 nm, 0.65 eV). In contrast, **CR2** in the presence of HCl exhibits a slightly structured fluorescence spectrum with the highest energy peak located at 410 nm and a Stokes' shift of only 3210 cm^{-1} (Figure 4), and is highly fluorescent ($\eta = 0.82$). Although **CR2**:2Mg^{2+} and **CR2**:2H$^+$ have similar absorption properties, the fluorescence spectra are drastically different. Clearly, the emission for **CR2**:2Mg^{2+} and **CR2**:2H$^+$ is from electronic states that are rather different in geometry and electronic character, as will be discussed further below.

The fluorescence lifetimes, τ, were measured for the three dyes with magnesium ion concentrations varying from 0 mM to 53 mM, and a dye concentration of ∼1 × 10^{-6} M. The uncomplexed dyes exhibited single-exponential fluorescence decays with lifetimes of 0.97 ns for **CN−DSB**, 0.83 ns for **CR1**, and 1.28 ns for **CR2** (see Table 1). Addition of 22 mM Mg^{2+} to a solution of **CN−DSB** reduced the lifetime slightly to 0.90 ns, but still gave a single-exponential behavior. Control experiments with ^{n}Bu$_4$N$^+$ (17 mM) resulted in single exponential decays and lifetimes very similar to those obtained for the pure dyes in acetonitrile. In contrast, the addition of magnesium to solutions of **CR1** resulted in a biexponential fluorescence decay, which is indicative of the presence of two fluorescent species in solution. One of the components has a fluorescence lifetime of 1.10 ns, whereas the second component has a lifetime of 420 ps. Similar lifetimes are obtained over the entire range of magnesium concentrations, but the relative amplitudes of the two components change with magnesium concentration and suggest that the 1.10 ns component is due to the free **CR1** and the 420 ps component to the **CR1**:Mg^{2+} species. The fluores-
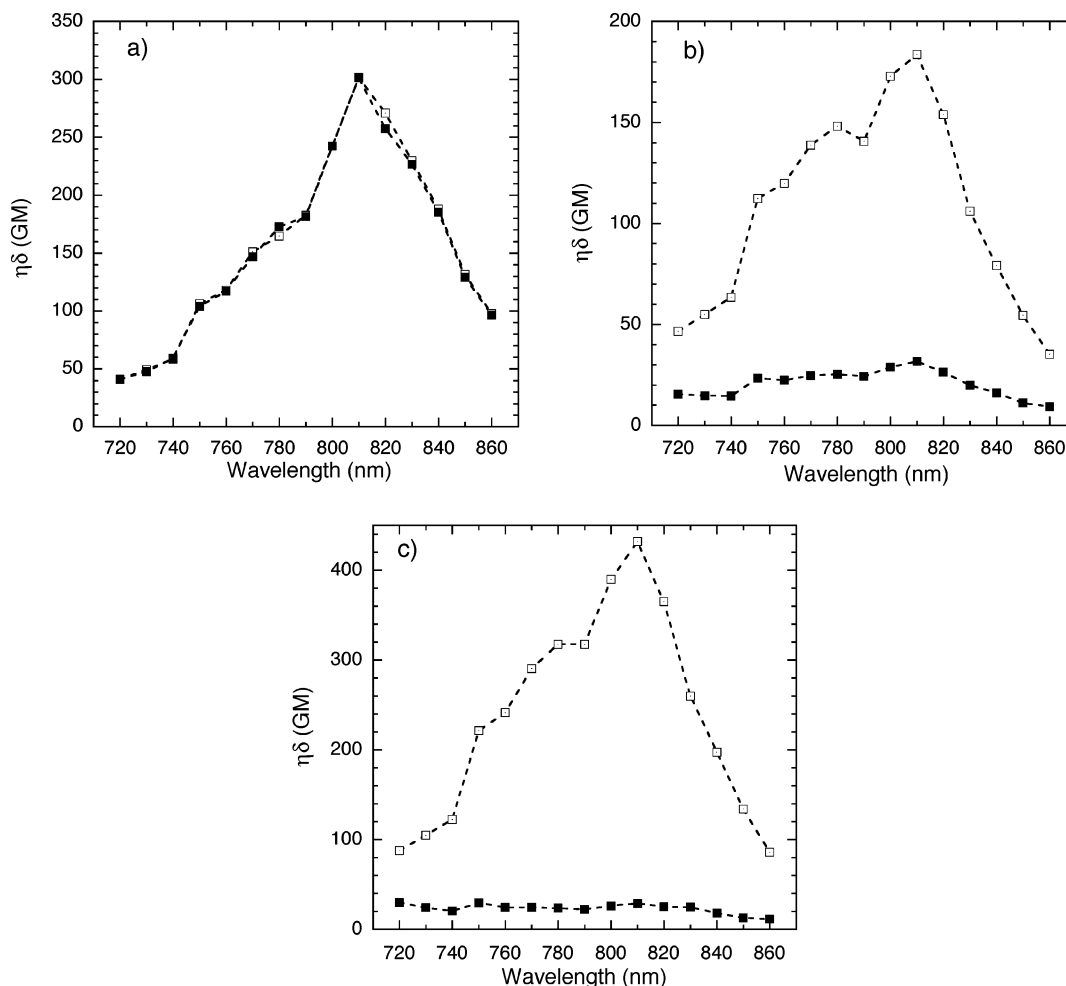
Figure 8. Two-photon action spectra of (a) **CN−DSB**, (b) **CR1**, and (c) **CR2** obtained using coumarin 307 as a reference. The open squares are data for the dyes in the absence of magnesium, the filled squares are data obtained with [dye] = 1×10^{-5} M and [Mg^{2+}] = 2 mM. The dashed lines are only a guide to the eye. The two spectra for **CN−DSB** are nearly overlapped.

cence decay of **CR2** in the presence of Mg^{2+} can be fit to a double exponential with lifetimes of 2.1 ns and 730 ps in the cases where the free dye concentration is less than 5% at equilibrium. At lower ion concentrations, where all three species are present in solution, a more complex decay is observed that can be fit to a triple-exponential decay function, with two lifetimes similar to those obtained in the double exponential case (and can be assigned to the two dye:ion complexes) and a third component corresponding to $\tau = 1.30$ ns, similar to the lifetime of the free dye. Analyzing the change in amplitudes of the components with magnesium concentration suggests that the 730 ps component should correspond to **CR2**:Mg^{2+} and the 2.1 ns component to **CR2**:2Mg^{2+}.

(v) Two-Photon Absorption Spectroscopy. Figure 8 shows the two-photon action spectra ($\eta\delta(\lambda)$) of **CN−DSB**, **CR1**, and **CR2** in solutions without Mg^{2+} and in solutions containing 2 mM Mg^{2+}, which is a concentration in the range of interest for physiological studies.[75] The three chromophores in the absence of Mg^{2+} ions have similar action spectra, with maxima at 810 nm and large peak two-photon absorption cross sections ($\delta \geq$ 1800 GM, Table 2). The differences in the action cross sections ($\eta\delta$) are mainly due to differences in the quantum yields of the three molecules, although δ values for the molecules with the

(75) Alberts, B.; Johnson, A.; Lewis, J.; Raff, M.; Roberts, K.; Walter, P. *Molecular Biology of the Cell*; 4th ed.; Garland Science: New York, 2002.

Table 2. Two-Photon Spectroscopic Parameters^a

sample	$\lambda^{(2)}$ (nm)	$\eta\delta_{max}$ (GM)	δ_{max} (GM)
CN−DSB	810	300	2500
CN−DSB (2 mM Mg^{2+})	810	300	
CR1	810	180	1800
CR1 (2 mM Mg^{2+})^b	810	26	
CR1 (65 mM Mg^{2+})^c	810	9.4	300
CR2	810	430	2150
CR2 (2 mM Mg^{2+})^d	810	29	
CR2 (55 mM Mg^{2+})^e	810	8.8	45

^{a} Excitation wavelength for the maximum of the two-photon absorption band ($\lambda^{(2)}$); two-photon action cross section ($\eta\delta_{max}$) and two-photon cross section (δ_{max}) at $\lambda^{(2)}$. ^{b} Equilibrium percentage: **CR1**:Mg^{2+} = 87%, **CR1** = 13%. ^{c} Equilibrium percentage: **CR1**:Mg^{2+} = 99.6%, **CR1** = 0.4%. ^{d} Equilibrium percentage: **CR2**:2Mg^{2+} = 34%, **CR2**:Mg^{2+} = 61%, **CR2** = 5%. ^{e} Equilibrium percentage: **CR2**:2Mg^{2+} = 94%, **CR2**:Mg^{2+} = 6%, **CR2** = 0.02%.

monoaza-15-crown-5-ether substituents are slightly smaller than that for the di-*n*-butylamino analogue, again suggesting that the azacrown is a slightly weaker donor group, consistent with the behavior observed in the linear absorption spectra.

The two-photon action spectra for **CN−DSB** and **CN−DSB** with Mg^{2+} are identical within experimental error. In contrast, for the chromophores with the crown ether binding groups, the presence of Mg^{2+} strongly affects the two-photon properties in the wavelength range between 720 and 860 nm. The two-photon

Figure 9. Two-photon absorption spectra obtained from quantum chemical calculations for **CR2** (solid line), **CR2**:2Mg²⁺ (squares and solid line), Me—CN—DSB (dashed line), and the model compound π—A—π shown in the figure (open circles and dashed line). δ is plotted as a function of excitation photon energy (1/2 of the transition energy).

Table 3. Results of Quantum Chemical Calculations[a]

	CR2	CR2:2Mg²⁺
E_{ge} (eV)	3.30	3.71
$E_{ge'}$ (eV)	3.81	4.30
$\Delta E = E_{ge} - E_{ge'}/2$ (eV)	1.40	1.56
M_{ge} (D)	11.8	11.3
$M_{ee'}$ (D)	17.7	11.6
δ_{max} (GM)	1240	560

[a] Reported are the total energy, E, of the one- and two-photon transitions (in the two-photon case, the photon energy is 1/2 E), the corresponding photon energy (1/2 E), the detuning energy (ΔE), the transition dipole moments, and the calculated peak two-photon cross sections for a damping $\Gamma_{ge'} = 0.1$ eV.

action cross section at 810 nm of **CR1** decreases by a factor of nearly seven in the presence of 2 mM Mg²⁺, resulting in an action cross section of 26 GM at 810 nm. For **CR2**, addition of magnesium ions (2 mM) decreases the action cross section by a factor of 15 at 810 nm, giving $\eta\delta = 29$ GM. In the samples used for these measurements, several species are present in solution. Using the binding constants obtained above, one can calculate that in the case of **CR1** with [Mg²⁺] = 2 mM, 87% of the dye is in the 1:1 complex and the remainder (13%) exists as free dye. In the **CR2** system, 5% of the chromophore is in the unbound state, 61% in a 1:1 complex, and 34% in the fully complexed 1:2 form.

To understand more fully the effect of the metal-ion complexation on the two-photon properties of the dye, measurements were also performed on solutions containing much higher concentrations of magnesium ions ($\geq$55 mM Mg²⁺), such that only the bound species were present in significant fractions. In this case (Table 2), for the mono-crown chromophore the solution contained 99.6% of **CR1**:Mg²⁺ complex and $\eta\delta$(810 nm) = 9.4 GM, corresponding to $\delta = 300$ GM. Similarly, for the bis-crown chromophore, for a solution containing 94% **CR2**:2Mg²⁺, 6% **CR2**:Mg²⁺, and 0.02% free **CR2**, $\eta\delta$(810 nm) = 8.8 GM, corresponding to $\delta = 45$ GM. This reveals the important point that the two-photon absorption cross section at the peak wavelength of the unbound species is reduced by about an order of magnitude upon ion binding. The observed reduction in δ may result from a decrease in the integrated two-photon cross section and/or from a shift in position of the two-photon absorption band. This issue will be addressed by quantum chemical calculations in the next section.

(vi) Quantum Chemical Calculations. To gain better insight into the effects of Mg²⁺ on the two-photon properties of the chromophores, quantum chemical calculations were performed on **CR2** and **CR2**:2Mg²⁺ as well as on two model compounds: a compound analogous to **CN—DSB** but with di(methyl)amino rather than di(n-butyl)amino donor groups (**Me—CN—DSB**), and a compound (π—A—π) in which the donor groups are replaced by hydrogen atoms (see Figure 9). The model compound π—A—π represents the limit of complete deactivation of the terminal electron donor groups and can be useful in assessing the extent to which the nitrogen electron donors in

CR2 are decoupled from the π-system upon complexation to Mg²⁺ ions. In general, the calculated energies (Table 3) of the two-photon state are higher than those observed experimentally, as has been noted previously[10] (partly due to overcorrelation of the ground state or inaccurate parametrization of the Hamiltonian for this type of molecule).

The calculated two-photon spectra for **Me—CN—DSB** and **CR2** are rather similar, with a two-photon absorption maximum at ~1.9 eV and $\delta_{max} \approx 1200$ GM (Figure 9). The π—A—π compound has a two-photon absorption maximum at 2.2 eV and δ_{max} just over 400 GM. Figure 9 also displays the calculated two-photon spectrum of the complexed species **CR2**:2Mg²⁺, which is shifted to higher energy by about 0.5 eV with respect to the uncomplexed compound, **CR2**. Additionally, the peak two-photon cross section is calculated to be smaller for the complex (560 GM) than for **CR2**. This is consistent with the experimental results, that show no evidence of a two-photon absorption band for **CR2**:2Mg²⁺ over the excitation wavelength studied which spans approximately 0.3 eV around the two-photon maximum for **CR2**. These findings indicate that the observed decrease in δ around 800 nm upon binding is primarily due to a shift of the two-photon absorption maximum to higher energies, with the decrease in the cross section playing a smaller role. The two-photon band position and strength for **CR2**:2Mg²⁺ are intermediate between the two limiting cases (**Me—CN—DSB** and π—A—π), but much closer to those for the π—A—π molecule. This is consistent with the crown nitrogen atoms being strongly, but not completely, decoupled from the π-system when magnesium ions are complexed by the crown.

Analysis of the calculated equilibrium configuration of **CR2**:2Mg²⁺ reveals that the nitrogen lone pairs of the terminal crown ethers lie almost in the same plane as the adjacent phenylene rings, such that their overlap with the π-orbitals on the phenylene carbon atoms is drastically reduced. In the **Me—CN—DSB** compound, if the coupling between the π-system and the dimethylamino donor is interrupted by rotating the nitrogen lone pairs by 90° relative to the terminal phenyl rings, the calculated two-photon spectrum is similar to the one for π—A—π, and characterized by a blue-shift of the band and a reduction in cross section with respect to the coupled case. This could suggest that the rotation about the C—N bond is the reason for the blue-shift in two-photon state. However, if the nitrogen lone pairs in **CR2**:2Mg²⁺ are forced by rotation about the C—N bond into a position that maximizes their overlap with the π-orbitals of the neighboring phenylene, the calculated two-photon spectrum is only slightly affected, remaining very similar to that for the calculated equilibrium configuration of **CR2**:2Mg²⁺. This indicates that the deactivation of the terminal donor groups

originates from their interaction with the Mg^{2+} ions and it is not due to a mere conformation change. The rotation of the donor group around the C−N bond can be viewed rather as a result of the deactivation of the donors and thus the decoupling of the nitrogen lone-pair from the π-system.

Calculations were performed also on **CR1** and its complex **CR1**:Mg^{2+}, but the obtained equilibrium conformations were not consistent with the results obtained for **CR2**:$2Mg^{2+}$ and the calculated cross sections failed to reproduce the experimentally determined ones. Additional work is under way to understand the origin of this discrepancy, which may be related to the different bonding situation that arises when there can be complexation to one or two Mg^{2+} ions, as discussed below. Calculations on a model compound for **CR1**:Mg^{2+}, namely a molecule with a distryrylbenzene backbone, two CN acceptor groups on the central phenylene and a dimethylamino donor group on only one of the outer rings (i.e., a molecule with general structure D−A−π), yielded results consistent with the experimental observations. From the calculations, we obtained a two-photon band centered at 2.07 eV and a peak two-photon cross section of 790 GM, values intermediate between those for **Me−CN−DSB** (with two donor groups) and π−A−π (with no donor groups). In the D−A−π model, we also find a weak two-photon band at the position of the main peak of **Me−CN−DSB** and that the one-photon state at 3.35 eV is two-photon active, as a result of the lack of an inversion center, with a cross section of 150 GM.

In the context of a simple three-level model and using eq 7, the changes in the magnitude of two-photon absorption cross section of **CR2** on ion binding can be attributed to (i) a significant reduction of the excited-state transition dipole moment ($M_{ee'}$) from 17.7 to 11.6 D, and (ii) an increase in the two-photon detuning term, ($\Delta E = E_{ge} - E_{ge'}/2$) from 1.40 to 1.56 eV. M_{ge} is calculated to be similar for the unbound and bound forms of the chromophore (11.8 and 11.3 D, respectively). The experimental estimates of M_{ge} for the lowest energy one-photon absorption band for **CR2** and **CR2**:$2Mg^{2+}$ are 9.6 and 8.7 D, respectively, suggesting a slightly larger decrease in M_{ge} upon binding than predicted by the quantum chemical calculations, but are, nonetheless, in reasonable agreement with the calculations.

(vii) Sensitivity and Contrast Figures of Merit. Two metrics often used to quantify the performance of ion sensing chromophores are sensitivity and contrast. The sensitivity (S) is the slope of a calibration curve (measured signal as a function of ion concentration) at the concentration of interest.[76] For **CR1**, the case in which there can be two emitting species in solution, the total one-photon or two-photon induced fluorescence signal (F) as a function of ion concentration ([M]) is

$$F([\text{M}]) \propto [\text{D}_t]\left(\eta_{\text{DM}}x_{\text{DM}}(\lambda)\frac{K_1[\text{M}]}{K_1[\text{M}]+1} + \eta_D x_D(\lambda)\frac{1}{K_1[\text{M}]+1}\right)$$

(9)

where x stands for ϵ or δ for the appropriate species in the one- or two-photon case, respectively. The other parameters have all been defined above. The sensitivity can then be obtained by differentiating eq 9 with respect to [M]

$$S([\text{M}]) = \frac{dF([\text{M}])}{d[\text{M}]} \propto \frac{[\text{D}_t]K_1}{(K_1[\text{M}]+1)^2}\{\eta_{\text{DM}}x_{\text{DM}}(\lambda) - \eta_D x_D(\lambda)\}$$

(10)

The expressions given by eqs 9−10 for one-photon and two-photon excitation have a different prefactor (not shown above), which depends on experimental and instrumental parameters. As evident in eq 10, S depends on the ion concentration, [M].

In the one-photon case, S is greatest at wavelengths for which the difference in $\eta\epsilon$ for the two species is largest. Figure 10a shows $\eta\epsilon$ for **CR1** and **CR1**:Mg^{2+} species as obtained from the global fitting analysis mentioned above, and the difference spectrum (term in brackets in eq 10; the absolute value of the difference is shown for simplicity). For one-photon excitation, the sensitivity is very small at 340 nm and greatest at 473 nm. In Figure 10c, S is plotted after normalization to -1 at [M] = 0 (notice that the normalized S does not depend on wavelength, as $-\{S([\text{M}])/S([\text{M}]=0)\} = -(K_1[\text{M}]+1)^{-2}$). S is largest (most negative) for small magnesium ion concentrations, and rapidly plateaus to zero at about 3 mM Mg^{2+}. A quasi-linear region of S can be identified for magnesium ion concentrations less than 0.02 mM ($K_1[\text{M}] \ll 1$), well below physiological concentrations. For two-photon excitation, the sensitivity curve after normalization is identical to that for the one-photon case. However, the actual scale of the two curves will be different once the prefactor for eq 10 is taken into account. The terms in parentheses in eq 10 for two-photon excitation are displayed in Figure 10b and suggest that the sensitivity for two-photon detection is largest at the peak of the two-photon band of the unbound species, consistent with a large shift of the two-photon band position. This treatment could be extended to **CR2**, once all the absorption and fluorescence characteristics of the three individual species are known.

The contrast describes the ability to distinguish between the two forms of the ion sensing chromophore and is typically defined as the difference in their fluorescence signals normalized to the signal from the native species: $(\eta_{\text{DM}} x_{\text{DM}} - \eta_D x_D)/(\eta_D x_D)$, i.e., $(\eta_{\text{DM}} x_{\text{DM}})/(\eta_D x_D) - 1$.[77,78] Since the contrast factor is dimensionless and does not depend on the excitation conditions, it should be possible to compare directly the cases of one- and two-photon induced fluorescence. As the fluorescence signal decreases on ion binding the contrast is negative and has a limiting value of negative one. The contrast has been calculated using the same limiting spectra shown in the sensitivity plots of Figure 10. As shown in Figure 11, both the one-and two-photon excitation of **CR1** result in a good contrast (>0.8 in absolute value) over a wide wavelength range (455−550 nm for one-photon excitation and 730−860 nm for two-photon excitation). Note that for an excitation wavelength of 340 nm, the contrast by one-photon excitation is zero, as the bound and unbound forms of the chromophore give the same integrated fluorescence signal. From the plots shown, it is apparent that one can obtain a somewhat higher contrast with two-photon excitation (-0.95) than with one-photon excitation (-0.90). This result shows that, in addition to the intrinsic advantages of two-photon absorption for imaging, it may be possible to design two-photon molecular sensors in which the

(76) Skoog, D.; Leary, J. J. *Principles of Instrumental Analysis*, 4th ed.; Saunders College Publishing: Fort Worth, 1992.

(77) Haugland, R. P. *Handbook of Fluorescent Probes and Research Products*, 9th ed.; Molecular Probes, Inc., 2002.
(78) Pawley, J. B., Ed. *Handbook of Biological Confocal Microscopy*; Plenum Press: New York, 1995.
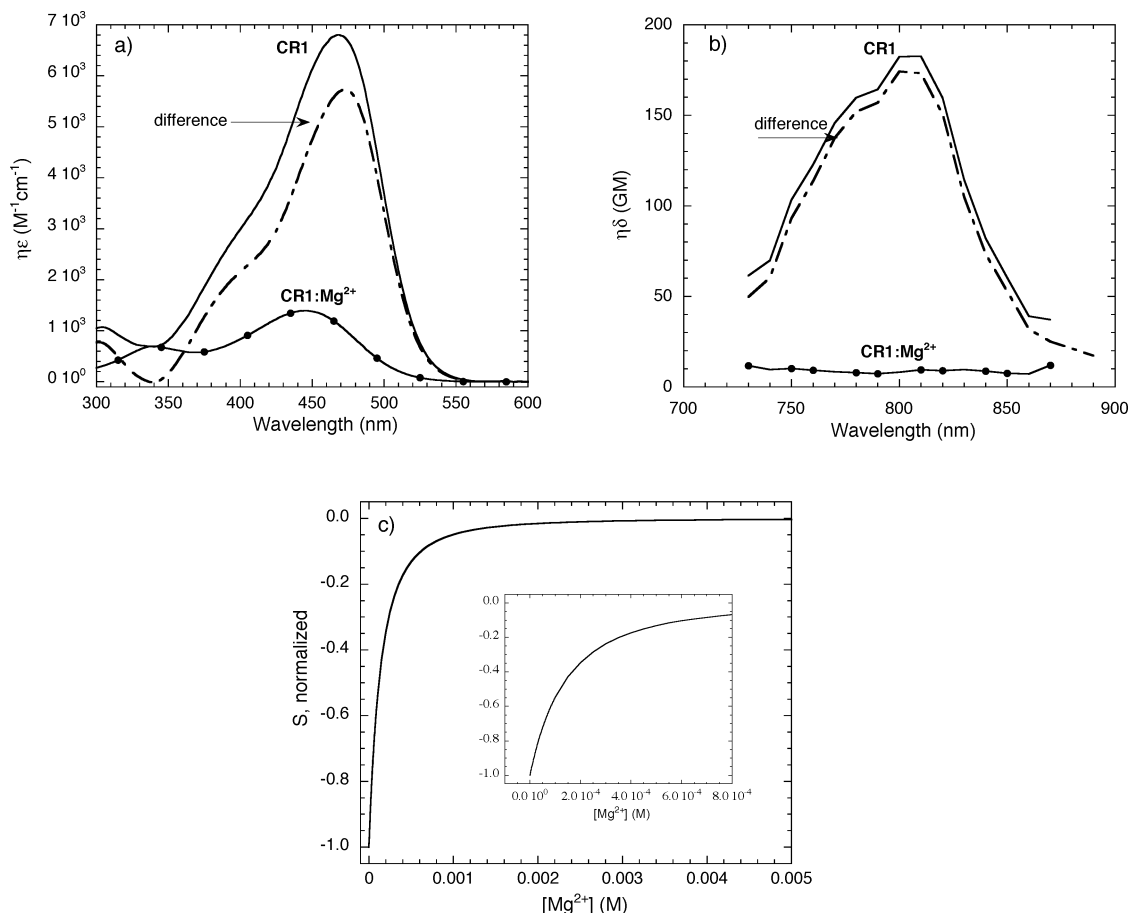
Figure 10. Sensitivity for **CR1**: (a) one-photon action spectra ($\eta\epsilon$), (b) two-photon action spectra ($\eta\delta$), and (c) sensitivity curve S (from eq 10) normalized to -1. The inset is a magnified view of the low concentration region. In plots (a) and (b), the absolute value of the difference is plotted for clarity.
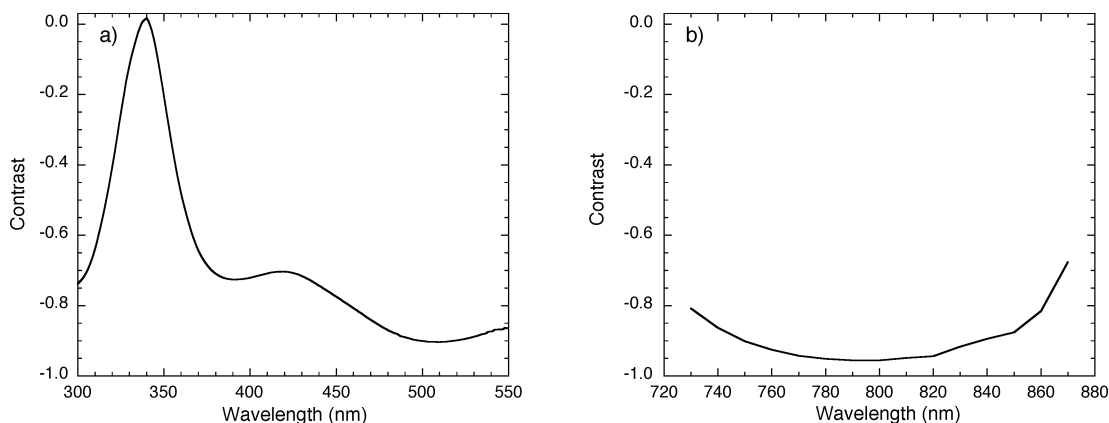
Figure 11. Contrast plots for **CR1**: (a) one-photon induced fluorescence and (b) two-photon induced fluorescence.

contrast between the bound and unbound forms is similar under one- and two-photon excitation conditions, if not slightly better in the two-photon case. In addition, for the two-photon excitation case, the contrast is larger than -0.8 over a $\sim$130 nm excitation region, allowing for considerable flexibility in the excitation wavelength.

These results differ from those of a recent study[5] in which the authors compared the response of commercially available ion sensing chromophores under one-photon and two-photon excitation conditions. There it was found that the sensitivity of calcium green and other chromophores was larger for one-photon than for two-photon excitation. For calcium green, changes in fluorescence intensity are due to electron transfer

quenching with binding, but the two-photon absorption cross section for that chromophore is not significantly modified by ion binding.[40] In cases where ion binding shifts the position of two-photon state or modulates $M_{ee'}$, affecting the two-photon but not the one-photon response, as for the molecules studied in this work, it is conceivable that molecular sensors could exhibit a larger optical response to ion binding under two-photon excitation conditions.

Discussion

The relatively small differences in the linear spectroscopic properties for the **CN−DSB**, **CR1**, and **CR2** in their unbound forms indicate that the mono-aza-crown-ether group is compa-

rable to but somewhat weaker as a donor relative to the di-*n*-butylamino group, and does not significantly perturb the electronic structure of the core of **CN−DSB**. All three compounds have large two-photon absorption cross sections in the near-IR region ($\delta > 1800$ GM). The changes in the spectral features of **CR1** and **CR2** in the presence of Mg^{2+} demonstrate that the aza-crown ether group retains the ability to bind magnesium ions when attached to the substituted distyrylbenzene backbone and that the dye:ion complexes exhibit very different spectroscopic properties from the free dyes, including a decrease in two-photon absorption cross section and significant shift in peak position. These changes can be understood in terms of the effect of ion binding on the degree of intramolecular charge transfer in the two-photon chromophore.

The optical studies indicate that the parent chromophore (**CN−DSB**) does not bind magnesium ions appreciably. The spectrophotometric titration of **CR1** with magnesium ions shows a behavior that is well described by the formation of a 1:1 dye:metal complex. The value of the binding constant ($K_1 = 3500$ M^{-1}) for **CR1** with Mg^{2+} is larger than values reported in the literature for the aza-15-crown-5-ether macrocycle attached to other chromophores (in acetonitrile). In cases where 1:1 complexes with Mg^{2+} are formed, the values of K_1 reported in the literature vary from 480 M^{-1} to 1500 M^{-1} for asymmetrically substituted donor−acceptor chromophores.[42,44,79] The spread in the values of the binding constant indicates that the strength of the interaction between the mono-aza-15-crown-5-ether and Mg^{2+} is modulated by the chromophore. The higher binding constant for **CR1** may be due to the D−A−D′ design motif. The absorption spectra of **CR2** in the presence of Mg^{2+} are consistent with a two-step complexation equilibrium in solution, involving the formation of chromophore:metal complexes with 1:1 and 1:2 stoichiometry. The binding constant for the formation of the **CR2**:Mg^{2+} complex ($K_1 = 6500$ M^{-1}) is approximately twice K_1 for **CR1**. This result can be explained by the fact that there are two binding sites per **CR2** molecule, thus doubling the effective concentration of binding groups, assuming that they are not interacting. K_{12}, the equilibrium constant for the formation of the **CR2**:$2Mg^{2+}$ species, is significantly smaller than K_{11}. For two independent binding sites, one would expect $K_{12} = K_{11}/4 = K_1/2$.[54] Our results indicate that there is a negative cooperativity between the two binding sites on a single molecule and that the binding of the second ion is significantly less favored that the first one. This could be explained by the fact that, after the first binding event, the electron density on the nitrogen on the other end of the molecule decreases, because of a larger partial charge transfer toward the electron accepting central portion of the molecule (the molecule now has effectively only one terminal donor group, but the same two CN acceptor groups). Thus, the interaction with a second ion is weaker. This change in charge distribution after ion binding is also consistent with the observation of a slight red-shift in the emission spectrum of **CR1**:Mg^{2+} and **CR2**:Mg^{2+} with respect to the unbound chromophores, indicative of a larger solvent reorganization energy due to a greater polarization of the chromophore after ion binding. A large difference in the two binding constants has also been reported for a symmetric bis-crown substituted diphenylpentadienone chromophore[47] and

a 9,10-bis(monoaza-15-crown-5)anthracene.[73] Examples of positive cooperativity can also be found in the literature.[80]

Our data are consistent with the following photophysical picture. Binding of an ion by the crown ether group involves coordination of the ion by all four oxygen atoms, as well as by the nitrogen atom in the crown. Upon binding, the nitrogen electron density is involved in the crown-ion interaction and is largely unavailable to the π-system, such that ion binding dramatically reduces the intramolecular charge transfer from the complexing nitrogen atom in the dye. This results in a blue shift of the absorption spectrum, as is seen in **CR1** and **CR2** upon addition of magnesium. The similarity between the absorption spectrum of **CR2**:$2Mg^{2+}$ and that of **CR2** in acidic conditions supports the hypothesis that, after binding, the nitrogens are largely decoupled from the π-system in the ground state. The blue-shift in the linear absorption of **CR1**:Mg^{2+} is smaller, as there is a remaining active electron donor coupled to the π-system, and an essentially donor−acceptor type electronic structure results. The spectrum of **CR1**:Mg^{2+} is quite similar to that of **CR2**:Mg^{2+}.

Once the chromophore is excited, relaxation processes occur over the lifetime of the excited state. There has been some debate in the literature regarding the strength of ion binding by the crown once the chromophore is in the excited state. It is generally believed that the binding strength of the macrocycle is lower in the excited state due to Coulombic repulsion. That is, upon excitation, the nitrogen atom involved in binding the ion becomes more positively charged, which repulses the cationic metal ion. It has been suggested that the nitrogen-ion bond is broken, and either the cation is ejected from the crown, or the cation becomes loosely coordinated by the oxygen atoms of the ring, with a solvent molecule completing the coordination of the ion.[81−86] Pump−probe spectroscopic studies of aza-crown ether systems and calcium ions have shown that the nitrogen-ion bond breaks in less than 10 picoseconds, and a reorganization of the coordination sphere of the ion occurs in 50 ps.[86]

The data reported here do not appear to support the complete photoejection of the ion from the crown group for the molecules we have studied. Solvatochromic studies of **CN−DSB** suggest that there is a larger quadrupolar moment in the excited state than in the ground state.[87] The increased positive charge density on the nitrogens that accompanies excitation will cause increased Coulombic repulsion with the positively charged metal ion in the crown and may cause destabilization of the nitrogen-ion bond. We observe that the fluorescence spectra of the bound and unbound species are different, indicating that the nature of the emitting states of the two species is different. This is particularly evident when comparing the emission spectra of **CR2**, **CR2**:$2Mg^{2+}$, and **CR2**:$2H^+$. The **CR2**:$2Mg^{2+}$ and **CR2**:

(79) Rurack, K.; Bricks, J. L.; Schulz, B.; Maus, M.; Reck, G.; Resch-Genger, U. *J. Phys. Chem. A* **2000**, *104*, 6171−6188.

(80) Marquis, D.; Desvergne, J.-P.; Bouas-Laurent, H. *J. Org. Chem.* **1995**, *60*, 7984−7996.
(81) Martin, M. M.; Plaza, P.; Dai Hung, N.; Meyer, Y. H.; Bourson, J.; Valeur, B. *Chem. Phys. Lett.* **1993**, *202*, 425−430.
(82) Martin, M. M.; Plaza, P.; Meyer, Y. H.; Badaoui, F.; Bourson, J.; Lefevre, J.-P.; Valeur, B. *J. Phys. Chem.* **1996**, *100*, 6879−6888.
(83) Lednov, I. K.; Ye, T.-Q.; Hester, R. E.; Moore, J. N. *J. Phys. Chem. A* **1997**, *101*, 4966−4972.
(84) Dumon, P.; Jonusauskas, G.; Dupuy, F.; Pée, P.; Rullière, C.; Létard, J.-F.; Lapouyade, R. *J. Phys. Chem.* **1994**, *98*, 10 391−10 396.
(85) Mathevet, R.; Jonusauskas, G.; Rullière, C.; Létard, J.-F.; Lapouyade, R. *J. Phys. Chem.* **1995**, *99*, 15 709−15 713.
(86) Jonusauskas, G.; Lapouyade, R.; Delmond, S.; Létard, J.-F.; Rulliére, C. *J. Chem. Phys.* **1996**, *93*, 1670−1696.
(87) Pond, S. J. K.; Rumi, M.; Alain, V.; Marder, S. R.; Perry, J. W., Unpublished results.

$2H^+$ species have very similar absorption properties, but very different emission properties. If the nitrogen atoms were still strongly coupled to the ion in the excited state, then one would expect the fluorescence of **CR2**:$2Mg^{2+}$ to be similar to that of **CR2**:$2H^+$. If the ions were completely ejected from the crown group on excitation, then the emission should be very similar to that of the free **CR2**. Neither of the extremes corresponds to the experimental findings. Thus, it appears that the emission for **CR2**:$2Mg^{2+}$ comes from a different geometric configuration. As the magnesium ion is smaller than the cavity size of the crown (the cavity size is 1.7−2.2 Å, the Mg^{2+} ionic diameter is 1.32 Å)[42] it is possible that a rearrangement of the ion in the crown takes place upon excitation to minimize the Coulombic repulsion. The geometric reorganization of the ion within the crown, and of the crown itself, in the excited state could explain the large Stokes' shifts observed for the dye:metal complexes. Geometric changes in the π-system of the chromophore when the ion and crown undergo rearrangement could also contribute to the relaxation energy. Additionally, the fluorescence lifetime decays show multiexponential behavior suggesting that more than one emitting species is present in solution and the amplitudes of the lifetime components generally change with magnesium ion concentration (i.e., as $[Mg^{2+}]$ increases, the lifetime component associated with the bound complex increases in amplitude). Thus, our results are consistent with a movement of Mg^{2+} away from the nitrogen atom and reorganization of the crown in the excited state, but do not support full photoejection of the ion.

The two-photon absorption cross sections of **CN−DSB**, **CR1**, and **CR2** in acetonitrile solution are all very large in the absence of magnesium ions. The disruption of the intramolecular charge transfer induced by ion binding dramatically affects the two-photon properties of the molecules, reducing $\eta\delta$ at the peak of the two-photon band of the unbound species by about a factor of 20 and decreasing δ by a factor of about six at 810 nm in the case of **CR1** in the high ion concentration regime. The **CR1**:Mg^{2+} complex is asymmetric and transitions to new two-photon allowed states outside the wavelength range studied here should be possible. For the **CR2** molecule, the change in the two-photon spectrum is even greater on ion binding, where $\eta\delta$ and δ decrease by a factor of nearly 50 at 810 nm in the 1:2 complex. As in the case of the linear absorption, where a large blue shift is observed, it is highly probable that a two-photon state exists at higher energy than the range examined. This is suggested by the quantum chemical calculations which show that the two-photon state for **CR2**:$2Mg^{2+}$ is 0.5 eV higher in energy than for **CR2**. The calculated value of δ_{max} for **CR2**:$2Mg^{2+}$ is less than one-half that of **CR2** and close to that of $\pi-A-\pi$. This clearly demonstrates that the changes in two-photon absorption are due to the reduced donating strength of the amine groups when an ion is bound by the receptor, which causes a shift in the state energy and a reduction in $M_{ee'}$.

Several difficulties in the use of these specific dyes as metal ion-sensing fluorophores should be pointed out. The aza-crown-ether binding group used in this study has been shown in the literature to bind magnesium, calcium, sodium, and several other ions and it does not possess the selectivity for one specific ion that would be desirable for most physiological studies. Additionally, this aza-crown receptor does not bind magnesium or calcium in the presence of water. However, even if these

dyes cannot be used directly in fluorescence microscopy applications in aqueous systems, the results presented here provide insight into how ion binding affects the one- and two-photon spectroscopic properties of D−A−D type chromophores and can aid in the design of a new generation of metal ion-sensing two-photon chromophores. For example, the use of crown ether groups of different sizes or with different donor atoms in the macrocycle could change the binding properties of the molecule and allow to achieve higher selectivity for a given cation. Alternatively, binding groups with different topology, either cyclic or acyclic, and ligating functionalities could be attached to the two-photon chromophore instead of the monoaza-15-crown-5 group used in this study. It is known that the BAPTA ligand (1,2-bis(*o*-aminophenoxy)ethane-*N,N,N′,N′*-tetraacetic acid) exhibits high selectivity for Ca^{2+} over Mg^{2+}.[88,89] Chromophores containing this ligand are commercially available (e.g., fura-2, indo-1, calcium green) and are widely used as indicators of intracellular Ca^{2+}.[77] However, BAPTA-based chromophores also bind strongly other heavy ions, such as Zn^{2+} and Cd^{2+}. Some chromophores containing the *o*-bis(carboxymethyl)amino carboxymethoxy phenyl ligating group possess large binding constants for Mg^{2+} (e.g., magnesium green and furaptra) and, although they still bind strongly Ca^{2+}, they can be used to study intracellular Mg^{2+}, due to the relatively high Mg^{2+} concentration. Some crown ethers and other macrocycles have also been used as magnesium ionophores for ion-selective electrodes.[90,91] In addition to the selectivity of the binding group, one must also consider other factors including: the magnitude of the binding constant relative to the range of ion concentrations that needs to be detected, as well as the magnitude of the two-photon cross section and the fluorescence quantum yield in the environment under study.

Conclusions

Two-photon chromophores substituted with one or two ion receptors have been demonstrated to exhibit changes in the one-photon and two-photon absorption and fluorescence properties with ion binding. In the aza-crown ether substituted compounds, where the nitrogen donor group is also a part of the ion binding group, binding to a magnesium ion results in the significant deactivation of the donor group and thus a decrease in the degree of intramolecular charge transfer in the chromophore, which is evidenced by a blue-shift and decrease in strength of both the one-photon and two-photon electronic transitions. The changes in the fluorescence properties of the molecule with ion binding indicate that the interaction between the crown ether and magnesium is weaker in the excited state than in the ground state, although it is unlikely that the magnesium ion is fully ejected from the crown.

The two-photon action spectra for **CR1** and **CR2** show strong two-photon signals in acetonitrile with $\eta\delta_{max} = 180$ and 430 GM, respectively, a significant improvement over currently available chromophores. It is also found that the contrast in detected signal between the **CR1** and **CR1**:Mg^{2+} species is somewhat larger and spans a larger bandwidth for two-photon excitation than one-photon excitation.

(88) Tsien, R. Y. *Biochem.* **1980**, *19*, 2396−2404.
(89) Grynkiewicz, G.; Poenie, M.; Tsien, R. Y. *J. Biol. Chem.* **1985**, *260*, 3440−3450.
(90) Suzuki, K.; Watanabe, K.; Matsumoto, Y.; Kobayashi, M.; Sato, S.; Siswanta, D.; Hisamoto, H. *Anal. Chem.* **1995**, *67*, 324−334.
(91) Choi, H.-J.; Lee, D.-H.; Park, Y. S.; Lee, I.-K.; Kim, Y.-C. *J. Incl. Phenom. Macrocycl. Chem.* **2002**, *43*, 15−18.

It can be concluded that a design scheme for ion sensing chromophores in which the ion binding event changes the degree of intramolecular charge transfer in the chromophore clearly can be applied to two-photon absorbing sensors. As δ depends not only on M_{ge}, but also on $M_{ee'}$ and this parameter has been shown to be strongly affected by ion binding, there is the potential for developing nonlinear molecular sensors with further enhanced sensitivity and contrast for use in two-photon laser scanning microscopy applications.

Supporting Information Available: Description of the global fitting procedure for the determination of the binding constants from absorption measurements (PDF). This materials is available free of charge via the Internet at http://pubs.acs.org.

JA049013T